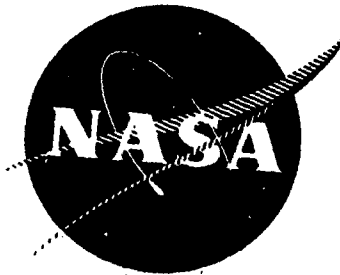


NASA CR-120889
N72-20768



STABILITY OF COMBUSTORS WITH PARTIAL
LENGTH ACOUSTIC LINERS

by

C. E. Mitchell, W. R. Espander and M. R. Baer

COLORADO STATE UNIVERSITY

prepared for

NATIONAL AERONAUTICS AND SPACE ADMINISTRATION

NASA Lewis Research Center

Grant NGR 06-002-095

Richard J. Priem, Project Manager

(NASA-CR-120889) STABILITY OF COMBUSTORS
WITH PARTIAL LENGTH ACOUSTIC LINERS C.E.
Mitchell, et al (Colorado State Univ.)
Mar. 1972 73 p

CSCI 21H

G3/28 23189 Unclas

N72-20768

NOTICE

This report was prepared as an account of Government-sponsored work. Neither the United States, nor the National Aeronautics and Space Administration (NASA), nor any person acting on behalf of NASA:

- A.) Makes any warranty or representation, expressed or implied, with respect to the accuracy, completeness, or usefulness of the information contained in this report, or that the use of any information, apparatus, method, or process disclosed in this report may not infringe privately-owned right; or
- B.) Assumes any liabilities with respect to the use of, or for damages resulting from the use of, any information, apparatus, method or process disclosed in this report.

As used above, "person acting on behalf of NASA" includes any employee or contractor of NASA, or employee of such contractor, to the extent that such employee or contractor of NASA or employee of such contractor prepares, disseminates, or provides access to any information pursuant to his employment or contract with NASA, or his employment with such contractor.

Requests for copies of this report should be referred to

National Aeronautics and Space Administration
Scientific and Technical Information Facility
P. O. Box 33
College Park, Md. 20740

1. Report No. NASA CR 120889		2. Government Accession No.		3. Recipient's Catalog No.	
4. Title and Subtitle Stability of Combustors with Partial Length Acoustic Liners				5. Report Date March 1972	
				6. Performing Organization Code	
7. Author(s) C. E. Mitchell, W. R. Espander and M. R. Baer				8. Performing Organization Report No.	
9. Performing Organization Name and Address Colorado State University Fort Collins, Colorado 80521				10. Work Unit No.	
				11. Contract or Grant No. NGR 06-002-095	
12. Sponsoring Agency Name and Address National Aeronautics and Space Administration Washington, D. C. 20546				13. Type of Report and Period Covered Contractor Report	
				14. Sponsoring Agency Code	
15. Supplementary Notes Project Manager, Richard J. Priem, Chemical Propulsion Division, NASA Lewis Research Center, Cleveland, Ohio					
16. Abstract An analytical technique for the evaluation of combustion stability in rocket motors with partial length acoustic absorbers is presented. The combustors considered in this work have concentrated combustion zones at the injector, finite mean flows, cylindrical cross sections, and acoustic liners of arbitrary length and impedance. Linear three dimensional oscillations in such combustion chambers are analyzed using an integral equation-iteration technique. Stability limits in terms of a combustion response factor are calculated for several values of Mach Number, length to radius ratio, liner impedance, liner length, liner location, and nozzle admittance. Results indicate that increasing liner length increases combustor stability substantially at low Mach Numbers but has a substantially smaller effect for larger Mach Numbers. Increasing Mach Numbers or length to radius ratio have destabilizing effects while liner location has only a minor effect on stability.					
17. Key Words (Suggested by Author(s)) Combustion instability Liquid rockets Acoustic absorbers				18. Distribution Statement Unclassified - unlimited	
19. Security Classif. (of this report) Unclassified		20. Security Classif. (of this page) Unclassified		21. No. of Pages 71	

PRECEDING PAGE BLANK

iii

Foreword

The research described herein, which was conducted at Colorado State University during the period December 1, 1969 to December 31, 1971 was supported by NASA Grant NGR 06-002-095. The work was done under the management of the NASA Project Manager, Dr. Richard J. Priem, Chemical Rockets Division, NASA Lewis Research Center.

ABSTRACT

An analytical technique for the evaluation of combustion stability in rocket motors with partial length acoustic absorbers is presented. The combustors considered in this work have concentrated combustion zones at the injector, finite mean flows, cylindrical cross sections, and acoustic liners of arbitrary length and impedance. Linear three dimensional oscillations in such combustion chambers are analyzed using an integral equation-iteration technique. Stability limits in terms of a combustion response factor are calculated for several values of Mach Number, length to radius ratio, liner impedance, liner length, liner location, and nozzle admittance. Results indicate that increasing liner length increases combustor stability substantially at low Mach Numbers but has a substantially smaller effect for larger Mach Numbers. Increasing Mach Number or length to radius ratio have destabilizing effects while liner location has only a minor effect on stability.

Nomenclature

a	- speed of sound
B_1, B_2	- quantities defined on Page A-2
C	- quantity defined on Page A-2
f_1, f_2	- functions defined on Page A-4
G	- Green's function
G_N	- modified Green's function defined on Page A-2
i	- unit imaginary = $\sqrt{-1}$
$\text{Im}()$	- imaginary part of ()
j	- positive integer
J_m	- Bessel Function of the first kind of order m
K	- absorber impedance
ℓ	- positive integer
L	- chamber length
M	- Mach Number
m	- positive integer
n	- positive integer or interaction index
\vec{n}	- outward unit normal vector
p	- pressure
\vec{q}	- velocity vector
R	- chamber radius
r	- radial length
\vec{r}	- position vector
\vec{r}_0	- source position vector
$\text{Re}()$	- real part of ()

S	- surface area of chamber
S_c	- surface area of acoustic liner
S_N	- surface area of nozzle exit plane
t	- time
u	- axial velocity
V	- chamber volume
v	- radial velocity
w	- circumferential velocity
z	- axial coordinate
β	- acoustic admittance
γ	- ratio of specific heats
η_N	- acoustic eigenvalue for mode N
θ	- circumferential coordinate
λ	- imaginary part of complex frequency
$\lambda_{\ell m}$	- root of $J'_m(\lambda_{\ell m}) = 0$
$\Lambda_{\ell mn}$	- normalizing constant defined on Page A-1
$\mu_{\ell n}^{(j)}$	- matrix discussed on Page A-3
ρ	- density
τ	- sensitive time lag
ϕ	- perturbation velocity potential
ψ	- normalizing constant defined on Page A-2
Ω_N	- acoustic eigenfunction for mode N
ω	- complex frequency of oscillation

Subscripts

- C - quantity evaluated on chamber cylindrical periphery
- i - injector quantity
- N - nozzle quantity
- o - mean value

Superscripts

- ' - perturbation quantity or derivative with respect to argument
- *
- ~ - chamber quantity with no absorber present
- ^ - designates particular mode integers chosen
- (j) - approximation of order j

Table of Contents

	Page
FOREWORD	iii
ABSTRACT	iv
NOMENCLATURE	v
INTRODUCTION AND SUMMARY	1
THEORY	3
Combustion Chamber Model	3
Basic Integral Equations	5
Solution of the Equations	6
RESULTS AND DISCUSSION	8
Stability Limit Results	10
Pressure and Velocity Profiles	13
CONCLUSIONS	17
REFERENCES	19
APPENDIX A - BASIC EQUATIONS	A-1
APPENDIX B - COMPUTER PROGRAM	B-1
Sample Calculation	B-3
Program Listing COMBADM	B-7

LIST OF ILLUSTRATIONS

Figure		Page
1	Rocket motor combustion chamber model with concentrated combustion	21
2	Neutral stability curves for successive ϕ approximations showing convergence	22
3	Neutral stability curves for various partial length liners - small M	23
4	Neutral stability curves for various partial length liners - larger M	24
5	Effect of decreasing K for various length liners .	25
6	Effect of liner length on neutral stability n, τ plot	26
7	Effect of Mach Number on neutral stability 1/3 length liner	27
8	Effect of liner impedance - 1/3 length liner . . .	28
9	Effect of L/R	29
10	Effect of liner placement - 1/4 length liner . . .	30
11	Effect of nozzle response	31
12	Pressure profiles for various length acoustic liners	32
13	Phase angle profiles for various length acoustic liners	33
14	Comparison of small matrix and large matrix pressure profiles	34
15	Radial velocity profiles for various length acoustic liners	35
16	Radial velocity profiles for various length acoustic liners	36
17	Radial velocity profiles for two different sizes of coefficient matrices	37
18	Radial velocity profiles for various length acoustic liners, $Z = 1.80$	38

INTRODUCTION AND SUMMARY

Acoustic liners designed for liquid rocket combustors usually cover only a fraction of the available wall area. It is therefore desirable to have an analytical means of predicting the stability behavior of combustors with acoustic absorbers of this type in addition to the existing analyses which are restricted to fully lined or unlined chambers. It is the purpose of this report to present an analytical technique of this type and to demonstrate its efficacy in predicting the stability characteristics of combustors with partial length liners. Priem (1) has shown that the combustion zone response, the nozzle admittance, and the mean flow in the chamber all can have strong effects on the frequency of chamber oscillations and on the linear stability of the oscillations both for unlined and fully lined chambers. In addition he showed that the axial dependence of the wave amplitude and phase was quite sensitive to the parameters mentioned above. Consequently, it is clear that in order to get a complete picture of the stability behavior of a combustor with a partial length liner, it is necessary to include mean flow, nozzle, and combustion zone response effects in any partial length liner analysis.

Because of the discontinuous boundary condition introduced into the problem by the partial length liner, standard separation of variables techniques will not work in the solution of the partial length liner problem. Instead it is necessary to transform the partial differential equations governing the chamber flow field into integral equations using

Green's theorem and a Green's function for the chamber. Similar transformations have been used previously by Culick (2) and Oberg (3).

These integral equations are then solved using an iterative technique and yield results in terms of stability limits and pressure and velocity waveforms. The effects of mean chamber Mach Number, nozzle impedance, liner impedance, length and location, chamber length to radius ratio and combustion zone response are then investigated using this iterative solution method.

THEORY

Combustion Chamber Model

The type of combustor considered in this work is assumed to have a concentrated combustion zone at the injector, to be of cylindrical cross section, to be terminated by a supercritical nozzle of known impedance and to have a finite mean flow (mean chamber Mach Number). An arbitrary fraction of the cylindrical periphery is assumed to consist of an acoustic liner of known impedance. The rest of the cylindrical chamber surface is assumed to have an infinite impedance. Figure (1) shows pictorially the type of combustor considered.

The response of the combustion zone mass generation rate is assumed to be pressure dependent only. Therefore, it can be represented using either a combustion response factor of the type used by Priem (1) or by the sensitive time lag (n, τ) model of Crocco (4). Both models will be used in interpreting the results of calculations performed in this work. Downstream of the combustion zone the gasdynamic field is assumed to be composed of a single component, calorically perfect gas. The flow is taken to be homentropic and irrotational.

Because of the irrotationality of the flow it is possible to combine the conservation equations into a single partial differential equation in terms of the velocity potential, Φ , following standard techniques. (See for example Ref. 1). If the oscillations are considered to be of small amplitude and periodic in time then $\Phi = Mz + \phi e^{i\omega t}$, where M is the mean Mach Number for the flow, z is the axial coordinate nondimensionalized by the chamber radius, ϕ is the perturbation velocity potential,

i is the square root of -1 , $\omega = \omega_R + i\lambda$ is the complex frequency of the oscillations and t is time nondimensionalized by the ratio of the chamber radius to the mean sound speed. With these definitions the linearized partial differential equation for ϕ can be written

$$\nabla^2 \phi + \omega^2 \phi = M^2 \frac{\partial^2 \phi}{\partial z^2} + 2i\omega \frac{\partial \phi}{\partial z} \quad (1)$$

Perturbation pressure and velocity are related to ϕ by the following expressions

$$p = -\gamma i \omega \phi - \gamma M \frac{\partial \phi}{\partial z}, \quad \vec{q} = \nabla \phi$$

The boundary condition on Equation (1) is $\nabla \phi \cdot \vec{n} = \beta p$ on the surface of the chamber (including injector plane and nozzle exit plane). β is the specific acoustic admittance of the bounding surface in question. On the portion of the cylindrical walls formed by the acoustic liner $\beta = \beta_c = 1/\gamma K$, where K is the specific acoustic impedance of the liner. At the combustion zone (injector plane) $\beta = \beta_i = M(\frac{1}{\gamma} - N)$, where N is the combustion response factor defined as $N \equiv \frac{\dot{m}^1}{M p}$ and γ is the specific heat ratio. \dot{m}^1 is the normalized perturbation in mass flux. If the time lag model is used $\beta_i = M[n(1 - e^{i\omega\tau}) - \frac{1}{\gamma}]$ where n is the interaction index and τ is the time lag. At the nozzle entrance plane $\beta = \beta_N$, the nozzle admittance. In this work the nozzle admittance used was either that for a short nozzle or the value obtained using the tabulated results of Crocco and Sirignano (5) for conical nozzles.

Basic Integral Equations

The single partial differential equation for the chamber flow (Equation (1)) and the boundary conditions discussed above can be transformed into two integral equations through the use of Green's theorem and the introduction of a Green's function for the chamber. The resulting equations are

$$\begin{aligned} \phi = & \Omega_N + \iint_S G_N(\vec{r}/\vec{r}_o) \beta[\gamma i \omega \phi + \gamma M \frac{\partial \phi}{\partial z}] ds_o \\ & + \iiint_V G_N(\vec{r}/\vec{r}_o) [M^2 \frac{\partial^2 \phi}{\partial z^2} + 2Mi\omega \frac{\partial \phi}{\partial z}] dV_o \end{aligned} \quad (2)$$

$$\begin{aligned} \omega^2 - \eta_N^2 = & \iiint_V \Omega_N (M^2 \frac{\partial^2 \phi}{\partial z^2} + 2Mi\omega \frac{\partial \phi}{\partial z}) dV_o \\ & + \iint_S \beta \Omega_N (\gamma i \omega \phi + \gamma M \frac{\partial \phi}{\partial z}) ds_o \end{aligned} \quad (3)$$

In Equations (2) and (3) the quantities Ω_N , η_N and G_N have the following meanings. Ω_N is one of the acoustic eigenfunctions for the chamber with no mean flow, combustion zone, liner, or nozzle. η_N is the eigenvalue for the frequency of oscillation associated with the eigenfunction Ω_N . G_N is a Green's function for the chamber represented as an eigenfunction expansion in the normal acoustic eigenfunctions of the chamber, with one specific eigenfunction (Ω_N) deleted from the triply infinite sum. The exact forms of the eigenfunctions, eigenvalues and Green's function are given in Appendix A.

Solution of the Equations

It was desired to obtain results in the form of stability limits in terms of either the real and imaginary parts of the combustion response factor or in terms of n and τ . In order to obtain results of this type Equation (3) was rewritten in the following form where β_i , the complex combustion admittance appears explicitly on the left hand side of the equation.

$$\beta_i = \frac{\omega^2 - \eta_N^2 - \iiint_V \Omega_N (M^2 \frac{\partial^2 \phi}{\partial z^2} + 2Mi\omega \frac{\partial \phi}{\partial z}) dV_o - \iint_{s-s_i} \beta \Omega_N (\gamma i \omega + \gamma M \frac{\partial \phi}{\partial z}) ds_o}{\iint_{s_i} \Omega_N (\gamma i \omega + \gamma M \frac{\partial \phi}{\partial z}) ds_o} \quad (4)$$

In this equation s_i is the injector plane surface area and $s-s_i$ is the rest of the chamber surface area.

Equations (2) and (4) above are sufficient to determine ϕ and β_i for given mean chamber operating conditions and geometry, and liner length, impedance, and location for a particular value of the complex frequency, ω . In order to obtain stability limits in terms of β_i , the equations must be solved for a range of frequency values. Stability limits in terms of the combustion response factor or n and τ are easily obtained using the expressions relating these quantities to β_i given earlier.

For a given frequency the following iterative solution method was followed. First, an initial guess for the form of ϕ and the value of β_i which will satisfy Equations (2) and (4) was made. In this work the ϕ and β_i resulting from solution of Equation (1) for the case of an unlined combustor were used as the initial approximations. This solution

is easily obtained using the technique of separation of variables since no discontinuous boundary condition is present in this case. These trial values for ϕ and β_1 were then substituted into the integrals on the right hand sides of Equations (2) and (4), resulting in first approximations for ϕ and β_1 for the lined chamber configuration. These first approximations were then themselves substituted into the right hand side integrals to produce improved approximations and so on. The iteration process continued until successive approximations were suitably invariant. A one per cent difference in successive values of β_1 was then taken to be the cut off point in most of the calculations performed, though this degree of accuracy is, of course, arbitrary.

RESULTS AND DISCUSSION

Calculations were performed for several values of Mach Number, chamber length to radius ratio, liner length, liner impedance, liner location and nozzle admittance. Results of those calculations in terms of both neutral stability limits and pressure and velocity profiles will be presented. Results for the first transverse mode of oscillation only will be discussed although some second and third transverse calculations have been done with similar results. Before giving these results a brief discussion of the convergence and accuracy of the iterative technique used will be presented.

It was found that the iteration technique converged in less than ten iterations to within the specified accuracy for almost all combinations of chamber design parameters investigated with two exceptions. The first of these was related to the magnitude of the damping effect of the liner. If this damping effect was too large (typically of the order of 100% decay per cycle or 1500 sec^{-1} damping coefficient) convergence was poor or did not occur at all. A rule of thumb seemed to be that if the ratio of liner length to liner impedance was less than about 0.50 convergence was good. Above this value difficulties began to occur. For a one third length liner, for example, the calculations were restricted to liners with impedances in excess of 0.60. This is clearly a very small impedance for practical liners so the restriction does not seem important for realistic calculations.

The other situation in which convergence was a problem was for the part of the neutral stability curves occurring in the transition between

various pure and combined modes of oscillation. That is, for example, for pure first transverse mode oscillations or for combined first transverse, first longitudinal oscillations convergence was good. For frequencies corresponding to oscillations not clearly first transverse or first transverse, first longitudinal, difficulties in convergence were experienced. These transition regions appear as loops on the neutral stability curves. Points along the loops can be found by improving the initial guess for ϕ and β_i with the inclusion of both modes in question, though convergence is still slower than usual.

Because the Green's function, G_N , is represented as an eigenfunction expansion, $\phi^{(j)}$, the j^{th} approximation for the velocity potential is also represented as a doubly infinite series in the r and z directions. (See Appendix A). Explicitly

$$\phi^{(j)} = \tilde{\phi} + \cos \hat{m}\theta \sum_{\ell=1}^{\infty} \sum_{n=1}^{\infty} \mu_{\ell n}^{(j)} J_m(\lambda_{\ell m} r) \cos \frac{n\pi z}{L}$$

where $\tilde{\phi}$ is the analytical solution for ϕ when no liner is present, \hat{m} signifies the particular transverse primary mode being considered (e.g., $\hat{m} = 1$ denotes the first transverse mode) and $\mu_{\ell n}^{(j)}$ is the coefficient matrix for the doubly infinite series. In order to carry out numerical calculations $\mu_{\ell n}^{(j)}$ must be finite in dimension. The largest matrix used in this work had 10 terms in the ℓ series (determining behavior in the radial direction) and 100 terms in the n series (determining behavior in the axial direction). Increasing matrix size beyond 10×100 can be shown to affect the stability limit results by less than 3%. Table 1 shows the errors in combustion response factor incurred when smaller

matrices are used as well as the number of iterations needed for convergence and the computer time required (CDC 6400). For the calculations performed in this study a 3 x 30 matrix was used in most cases. The effect of matrix size on pressure and velocity profiles will be discussed later.

Stability Limit Results

Convergence of the technique in terms of shape and location of the linear stability curve is shown in Figure (2). $\text{Re}(N)$ and $\text{Im}(N)$ are the real and imaginary parts of the combustion response factor, M is the mean Mach Number, L/R is the length to radius ratio for the chamber, K is the acoustic impedance of the liner, and G is the acoustic response of the nozzle. A value for G of 0.9166 corresponds to a short nozzle response. The normalized liner length is given by X . A value of X of 2.7 indicates a fully lined chamber if $L/R = 2.7$. The nondimensional frequency ω/ω_0 is the parameter used along the curves. ω is the actual chamber frequency; ω_0 is the frequency of the acoustic first transverse mode for no combustion, mean flow, or liner. Progressing along any of the curves in the direction of increasing frequency, regions to the right of the curve are linearly unstable while regions to the left are linearly stable. For the example chosen it is seen that there is no change in the stability limit location after five iterations. It is to be noted that the first and second approximations are noticeably in error even though $M = 0.10$ and the usual linear or second order expansions in Mach Number might be expected to be accurate.

Figure (3) shows the effect of varying liner length on the stability of a low mean Mach Number chamber. It is readily seen that increasing the liner length increases the region of linear stability. (The neutral stability curves shift to the right with increasing X). Moreover, this increase in stability with liner length is seen to be almost linear for the Mach Number being considered. In Figure (4) which is the same type of plot, the effect of increasing the mean Mach Number is seen. For this figure all chamber parameters are the same with the exception of the mean Mach Number which has been increased from 0.1 to 0.33. It can be seen that "loops" are introduced into the neutral stability curves. These coincide with the appearance of combined modes of oscillation and have been observed previously by Priem (1) and others. The stabilizing effect of adding a liner is diminished with the increase in Mach Number. As can be seen, the shift to the right caused by the addition of a liner is considerably less than it was for the case of the low Mach Number chamber in Figure (3). Finally it is seen from Figure (4) that adding more liner is also less effective than was the case for $M = 0.1$. Indeed, a $1/3$ length liner provides half the stability improvement of a full liner and a $2/3$ length line provides essentially the same stabilizing effect as a full liner. Figure (5) shows the effect of decreasing the impedance (increasing the damping effect) of the liner while keeping all other parameters at the values they had in Figure (4). Two facts are apparent from the figure. First the linear stability is improved considerably as all three liner neutral stability curves are shifted to the right from their position in Figure (4). Second, the effect of liner length has become even less

important. Indeed, there seems to be little difference between a $1/3$, $2/3$ and full liner as far as overall stability improvement. These conclusions are verified and perhaps clarified in Figure (6). This figure shows, for the same chamber parameters and the same liners, neutral stability plots on the n, τ plane. n is the interaction index and τ the sensitive time lag of Crocco's Sensitive Time Lag Model (4). Frequency increases from the right to the left along the curves. The region above any neutral stability curve is a region of linear stability, the region below a region of linear stability. Thus, shifting a neutral stability curve upward increases stability. Figure (6) shows that for lower frequencies the longer liners are slightly more stabilizing, but that for higher frequencies (e.g., combined 1st transverse 1st longitudinal) the shorter liner is actually slightly more effective. Figures (7) and (8) show, respectively, the effect of increasing Mach Number for a fixed liner impedance and length and the effect of decreasing the liner impedance for fixed Mach Number and liner length. It is clear from the figures that increasing the Mach Number is destabilizing while decreasing the liner impedance provides a stabilizing effect.

Figure (9) shows the effect of increasing the chamber length to radius ratio on the chamber's stability. It can be seen that increasing L/R provides a substantial destabilizing effect. Examination of Figures (7) and (8) indicate that increasing either L/R or M increases the number of combined modes possible. Figure (10) demonstrates the influence of liner location. A $1/4$ length liner is located at various positions in the chamber and the neutral stability curve determined for each

location. If $X_1 = 0$ the liner is at the injector end, if $X_1 = 0.75$ the liner is at the nozzle end, and if $X_1 = .40$ the liner is in the center of the chamber. It can be seen that there is little difference in overall effectiveness between $X_1 = 0.0$ and $X_1 = 0.40$ but that $X_1 = 0.75$ is somewhat less effective. The influence of nozzle response on the neutral stability limits is shown in Figure (11). Two types of nozzles are compared both with and without $1/3$ length liners. One of the nozzles is a "short" nozzle, the other is a conical nozzle of the type analysed by Crocco and Sirignano. For the short nozzle the nozzle admittance is not a function of frequency and provides a small damping effect. For the conical nozzle β_N is a function of ω , and, according to the Crocco-Sirignano calculations, provides a small driving effect in the frequency range of interest. Comparison of the short nozzle and conical nozzle stability limits for either lined or unlined chambers indicates that, as is to be expected, the chamber with the short nozzle is always more stable than the chamber with the conical nozzle. It is important to observe that the stability improvement caused by the addition of a liner is approximately the same for both types of nozzles. This means that stability improvement predictions for lined chambers with short nozzles are likely to also apply for other types of nozzles.

Pressure and Velocity Profiles

The perturbation pressure and velocity were calculated as a function of spatial coordinates using the relationships given in Appendix A. Results are presented for a frequency value (ω/ω_0) of 0.90. Figure (12)

is a plot of relative pressure amplitude (ratio of pressure amplitude at a particular radial and axial location to the pressure amplitude at the injector for the same radial location) as a function of axial length for the standard chamber with no liner, with a 1/3 length liner ($X = 0.9$) and with a full liner ($X = 2.7$).

For the unlined chamber the amplitude continuously decreases from injector to nozzle. For the fully lined chamber the amplitude decreases very rapidly near the injector and then maintains a more or less constant value for the rest of the chamber. The 1/3 length liner causes a more rapid decrease in amplitude near the injector than in the case of the unlined chamber, but not as pronounced as in the case of the fully lined chamber. Approximately at the end of the lined portion the 1/3 length liner curve starts to follow the unlined chamber curve and converges to it as the nozzle end is approached.

Figure (13) shows the phase angle difference between the injector and a given location for a given wave. The same chamber configuration and liners are considered as in Figure (12). It can be seen that for the unlined chamber the wave downstream of the injector always leads the wave at the injector with the lead in general increasing with axial length. For the chamber with a 1/3 length liner the phase angle curve is qualitatively similar except near the injector where a region of lagging occurs. The fully lined chamber presents a quite different wave shape with the wave in the center of the chamber lagging the wave at both the injector and nozzle. The effect of $\mu_{\ell n}^{(j)}$ matrix size on the relative pressure amplitude curve is shown in Figure (14). The large

matrix is 10 x 30 and the small matrix is 3 x 30. The curves are qualitatively very similar though the small matrix predicts a somewhat more rapid decrease in pressure amplitude than does the large matrix.

The radial velocity as a function of axial length at a radial location 0.90 of the chamber radius is shown in Figure (15) for the same chamber with the same three liner configurations. Velocity values were calculated assuming that the arbitrary amplitude factor for the velocity potential, ϕ , was unity in the case where no liner was present. It can be seen that, as might be expected, (since v_r at the wall $\neq 0$) the addition of a full length liner increases the radial velocity above the value with no liner present at every axial location. The 1/3 length liner causes an even greater increase in v_r over the lined portion but v_r gradually tends toward v_r for the unlined chamber as the nozzle is approached.

The dependence of the radial velocity on radius for an axial location 0.45 of the chamber radius is shown in Figure (16). As the wall is approached ($r = 1$) the radial velocity increases substantially above the value for the unlined chamber and then decreases rapidly to zero both for the 1/3 length liner and the full liner. The 1/3 length liner produces slightly larger radial velocities than does the full length liner. Because of the use of the Green's Function Technique, the wall boundary condition $v_r \neq 0$ cannot be satisfied exactly at the wall except in the limit as an infinite number of terms are retained in the radial direction in the matrix for $\mu_{\ell n}^{(j)}$.

A comparison of small matrix (3 x 30) to large matrix (10 x 100)

results near the wall is shown in Figure (17). As the number of terms kept is increased a better satisfaction of the wall boundary condition is experienced. It is to be recalled that the increase in accuracy in the determination of combustion response factors improved by less than 5% in going from the 3×30 to 10×100 matrix. Therefore, it seems that the detailed satisfaction of the wall boundary condition is relatively unimportant in obtaining neutral stability results. Figure (18) is similar to Figure (16) except that the axial location has been changed to 1.8 of the radius. Here the wall is unlined for the $1/3$ length liner chamber. It can be seen that for this case the fully lined chamber radial velocity is larger than the other two near the wall and that the curve for the $1/3$ lined chamber is considerably closer to the unlined chamber curve than it was in Figure (16).

CONCLUSIONS

An analytical method for predicting the linear stability behavior of rocket combustors with partial length liners has been presented. It has been shown that the method is applicable over a wide range of chamber and absorber design parameters. Calculations performed indicated that the following general characteristics of the stability of combustors with partial length liners are to be expected.

1. An increase in the mean flow Mach Number provides a destabilizing effect for a given chamber and reduces the stability improvement provided by an acoustic liner.
2. Increasing the chamber length to radius ratio results in the same type of destabilizing effects as increasing the Mach Number.
3. Increasing liner length as a means of increasing stability is most effective at high liner impedances and low Mach Numbers. For large Mach Numbers and small impedances partial length liners can be as effective as full length liners.
4. Decreasing liner impedance for a given liner length always provides a marked increase in stability.
5. Location of a partial length liner is not very important, though liners located at the nozzle tend to be slightly less effective than if located elsewhere.
6. A wide range of frequencies of oscillation (including combined modes) is possible with a partial length liner

in place. The liner is more effective as a damping device (even if its impedance is fixed) at some frequencies than it is at others.

REFERENCES

1. Priem, R. J. and Rice, E. S., "Combustion Instability with Finite Mach Number Flow and Acoustic Liners," NASA TMX-52412, 1968.
2. Culick, F. E. C., "Acoustic Oscillations in Solid Propellant Rocket Chambers," *Astronautics ACTA*, Vol. 12, No. 2, 1966, p. 113-124.
3. Oberg, C. L. and Kuluva, N. M., "Acoustic Liners for Large Engines," Final Report NASA Contract 21345, Rocketdyne Report No. K-7792, 1969.
4. Crocco, L., and Cheng, S. I., Theory of Combustion Instability in Liquid Propellant Rocket Motors, Agardograph No. 8, Butterworth, 1956.
5. Crocco, L., and Sirignano, W. A., "Behavior of Supercritical Nozzles Under Three-Dimensional Oscillatory Conditions," Agardograph 117, 1967.

Size of Coefficient Matrix	Combustion Response Factor (N)	Error w.r.t. 10 x 100 Coefficient Matrix			Time per Iteration (sec) *	Number of Iterations for 1% Convergence	Time for Convergence (sec)
		Real (%)	Imaginary (%)	Modulus (%)			
10 x 100	0.7701 - 0.89751				87.7422	6	526.4520
3 x 100	0.7194 - 0.86281	6.6	3.9	4.2	20.0964	6	120.5784
10 x 30	0.7624 - 0.87841	1.0	2.1	1.7	22.5742	6	135.4453
3 x 30	0.7336 - 0.85361	4.7	4.9	4.0	1.8777	7	13.1439
2 x 30	0.8352 - 0.88731	-8.5	1.1	-3.0	1.2684	14	17.7576
1 x 30	0.7132 - 0.82471	7.4	8.1	7.8	0.6362	6	3.8172
3 x 10	0.7720 - 0.82051	-0.2	8.6	3.9	0.3505	8	2.8040
2 x 10	0.8679 - 0.84491	-12.7	5.9	-2.4	0.2270	7	1.5890
1 x 10	0.7525 - 0.79201	2.3	11.8	7.6	0.1245	8	0.9960
3 x 5	0.8333 - 0.76261	-8.2	15.0	3.7	0.1625	18	2.9250
2 x 5	0.9342 - 0.78991	-21.3	12.0	3.5	0.1053	9	0.9477
1 x 5	0.8174 - 0.73111	-6.1	18.5	7.3	0.0602	10	0.6020
3 x 3	0.9078 - 0.66541	-17.9	25.9	4.8	0.0890	9	0.8010
2 x 3	1.0130 - 0.66391	-31.5	26.0	2.4	0.0638	5	0.3190
1 x 3	0.8991 - 0.62811	-16.6	30.0	7.3	0.0373	12	0.4476

* Note: Computer was a CDC 6400

Table 1 - Effect of Matrix Size

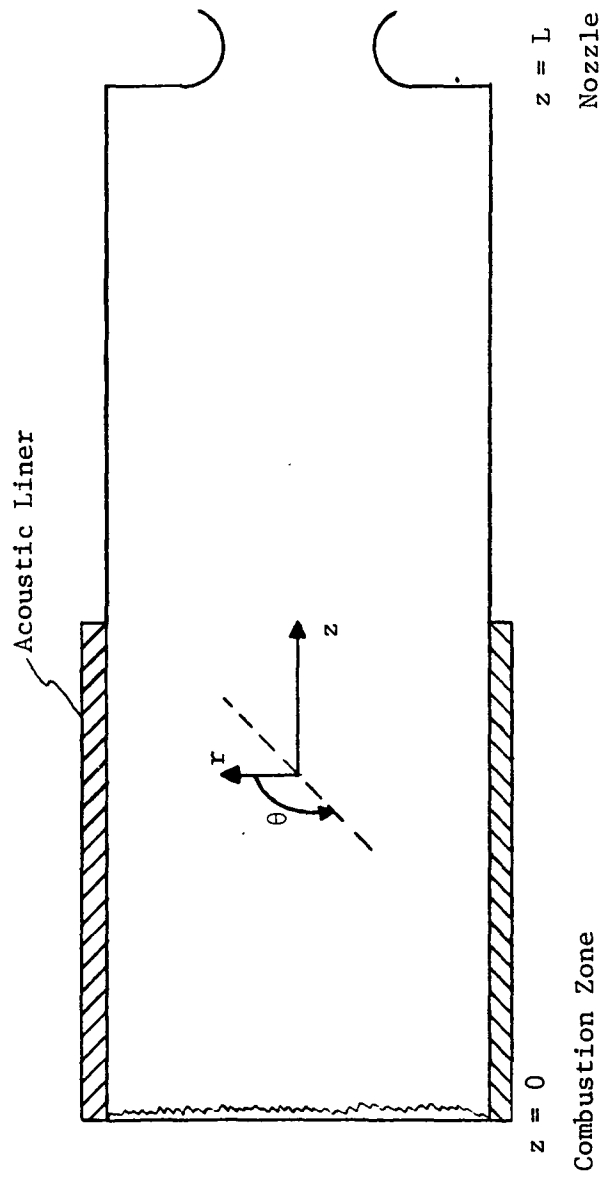


Figure 1 Rocket motor combustion chamber model with concentrated combustion.

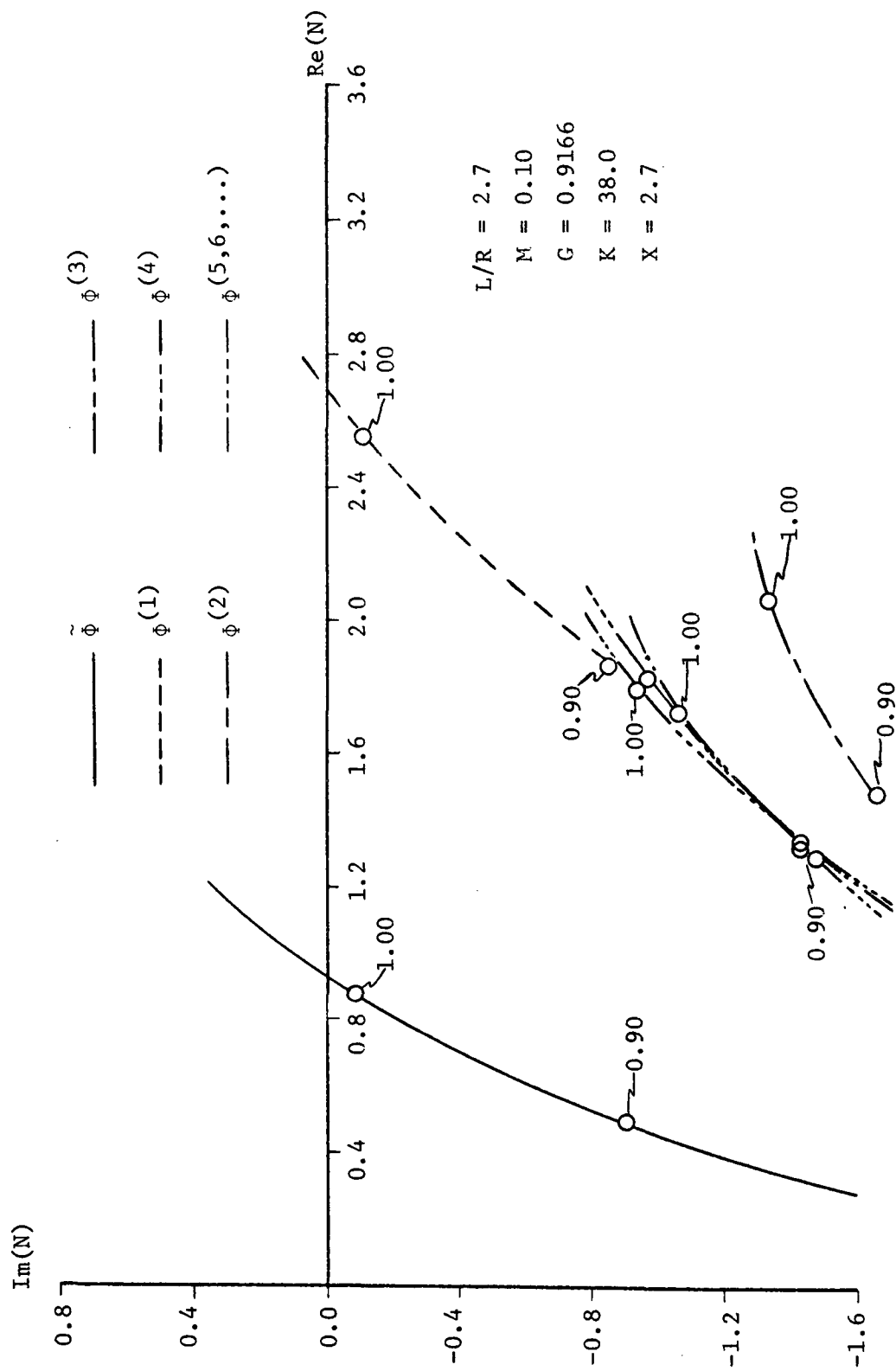


Figure 2 Neutral stability curves for successive ϕ approximations showing convergence.

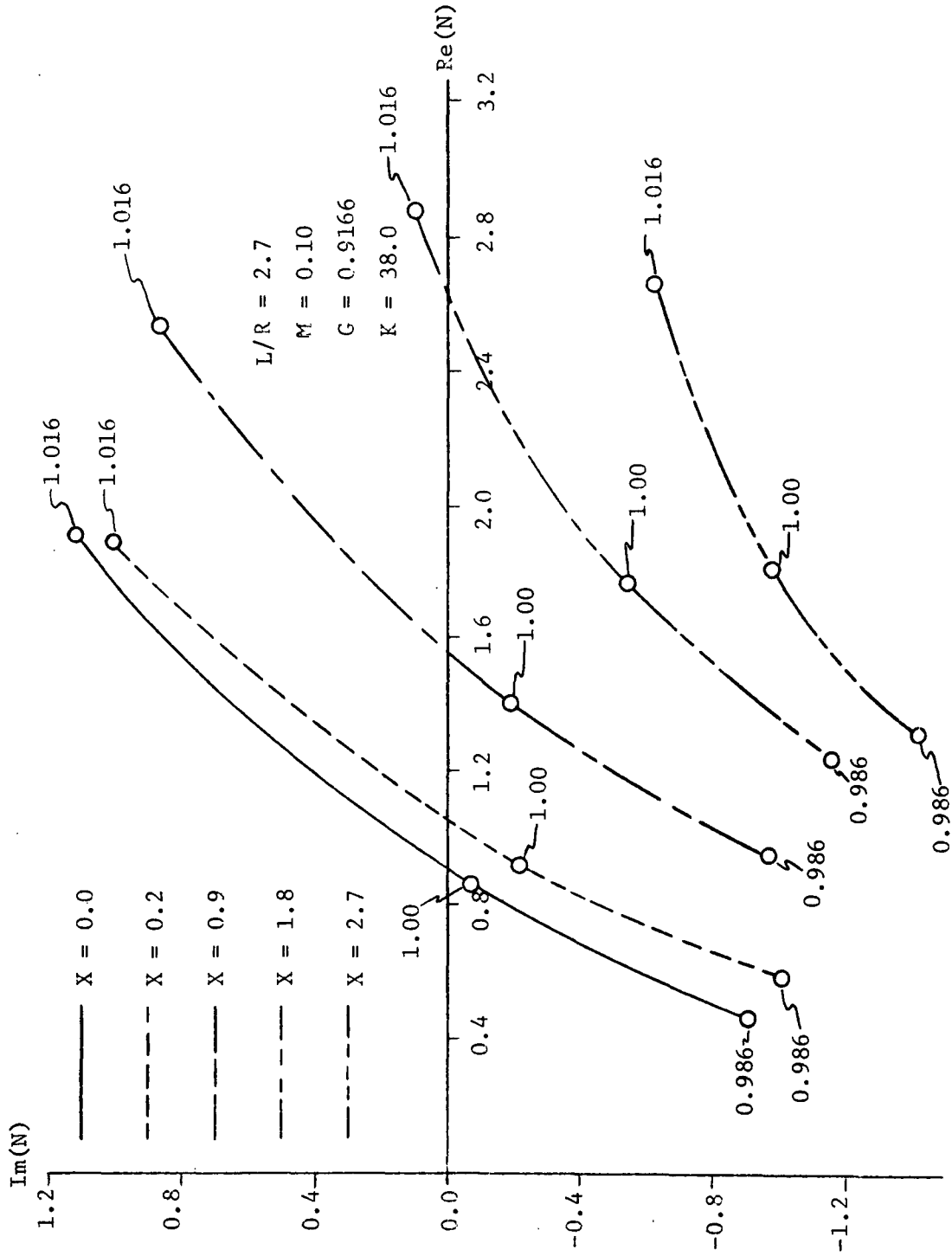


Figure 3 Neutral stability curves for various partial length liners - small M .

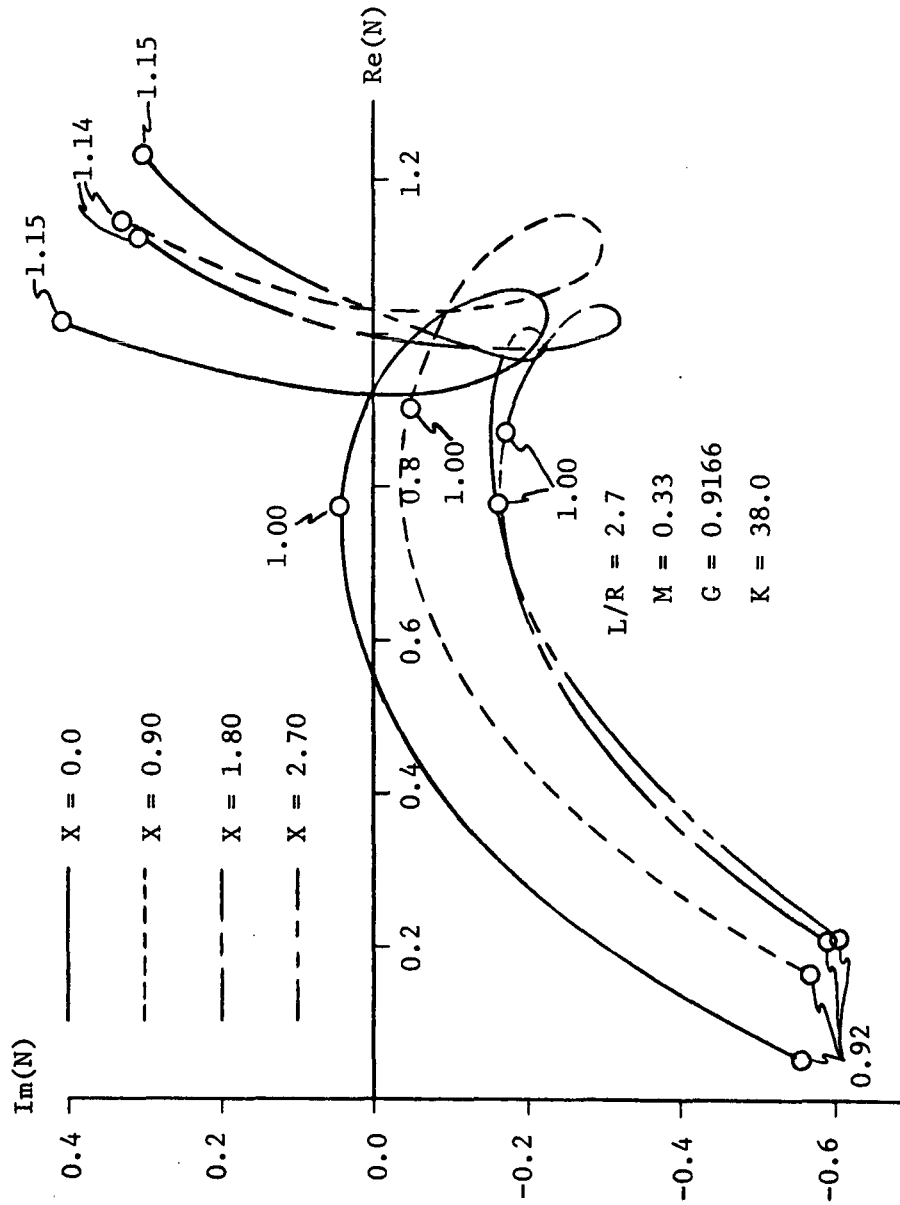
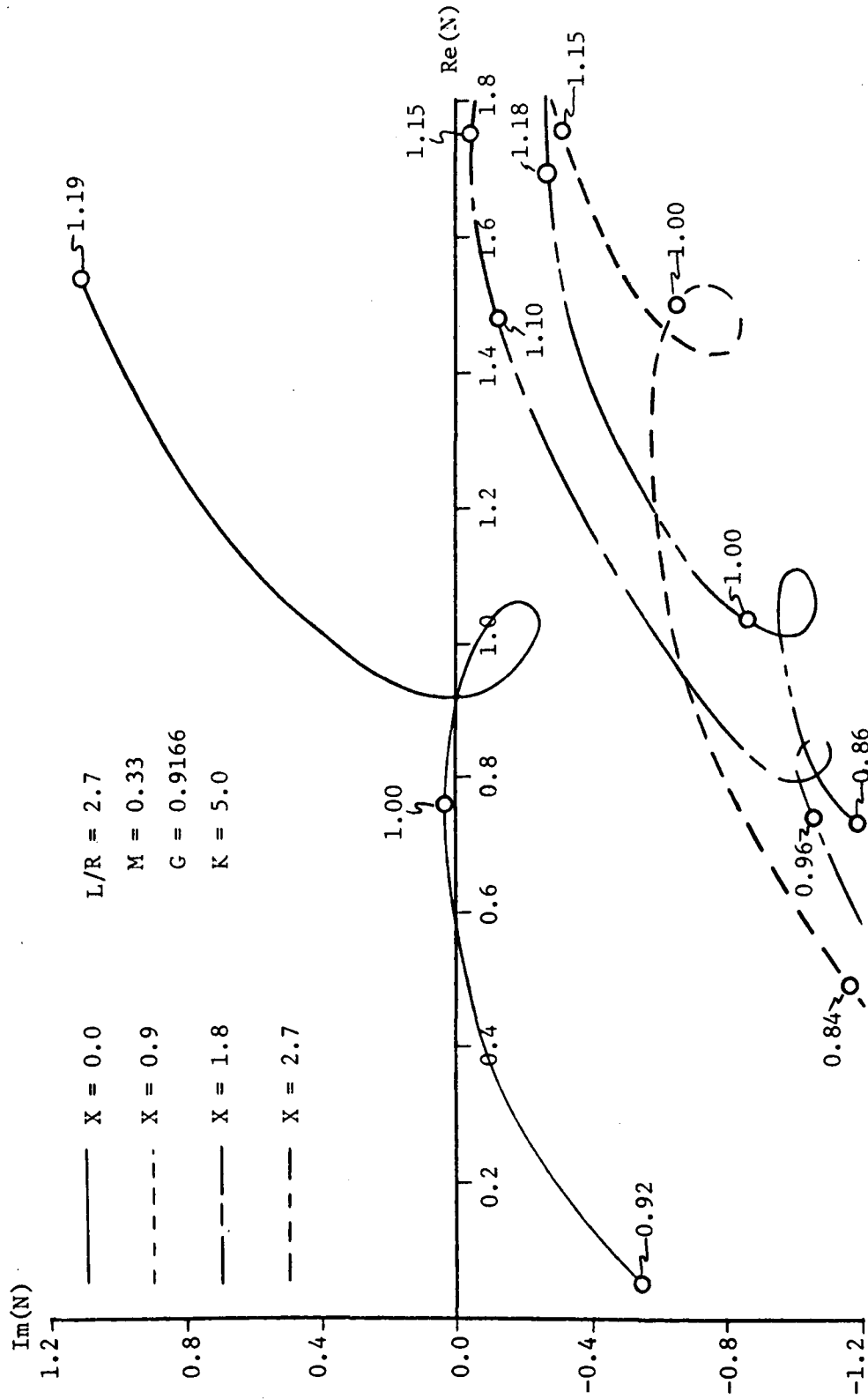
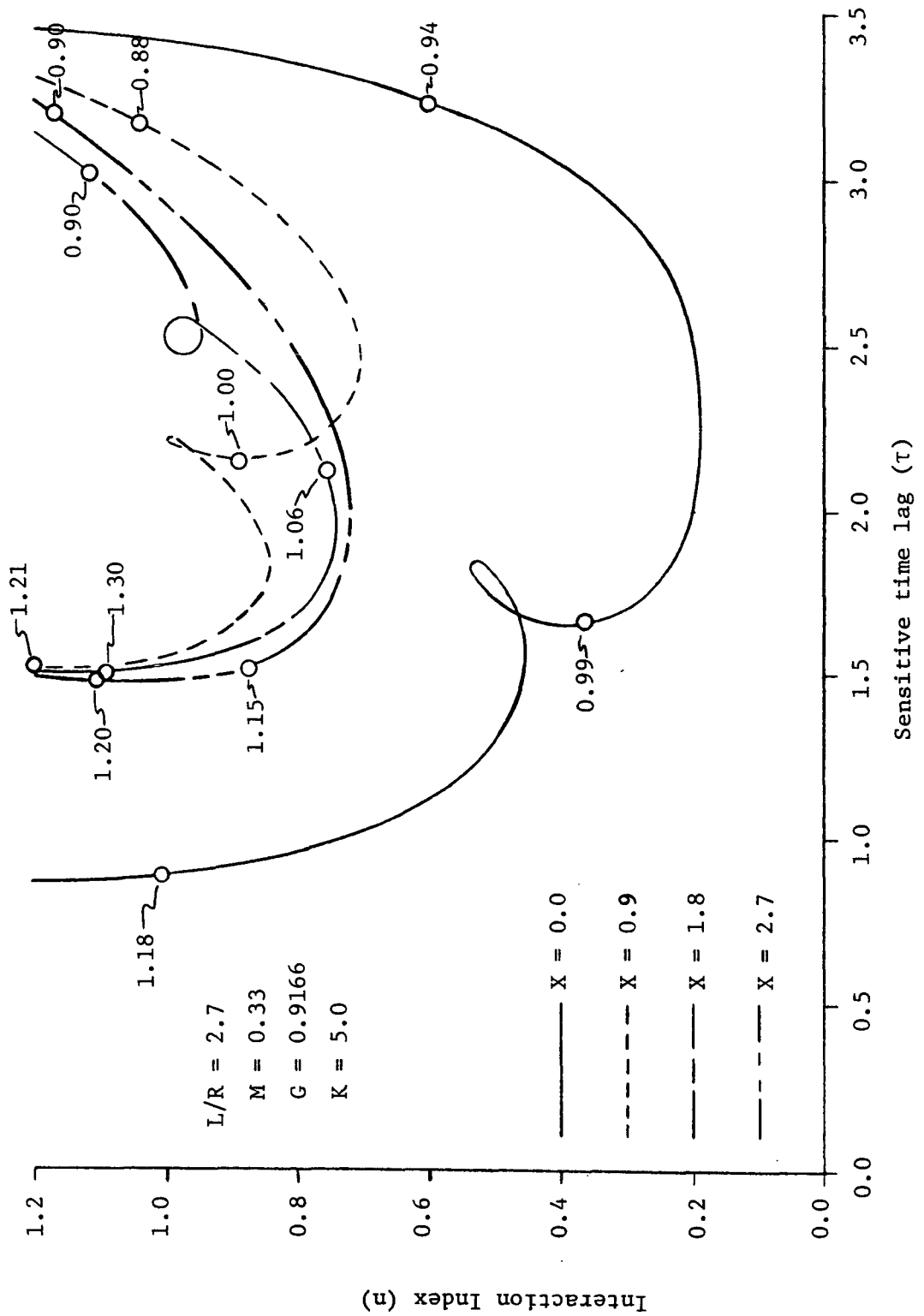


Figure 4 Neutral stability curves for various partial length liners - larger M.

Figure 5 Effect of decreasing K for various length liners.

Figure 6 Effect of liner length on neutral stability - n, τ plot.

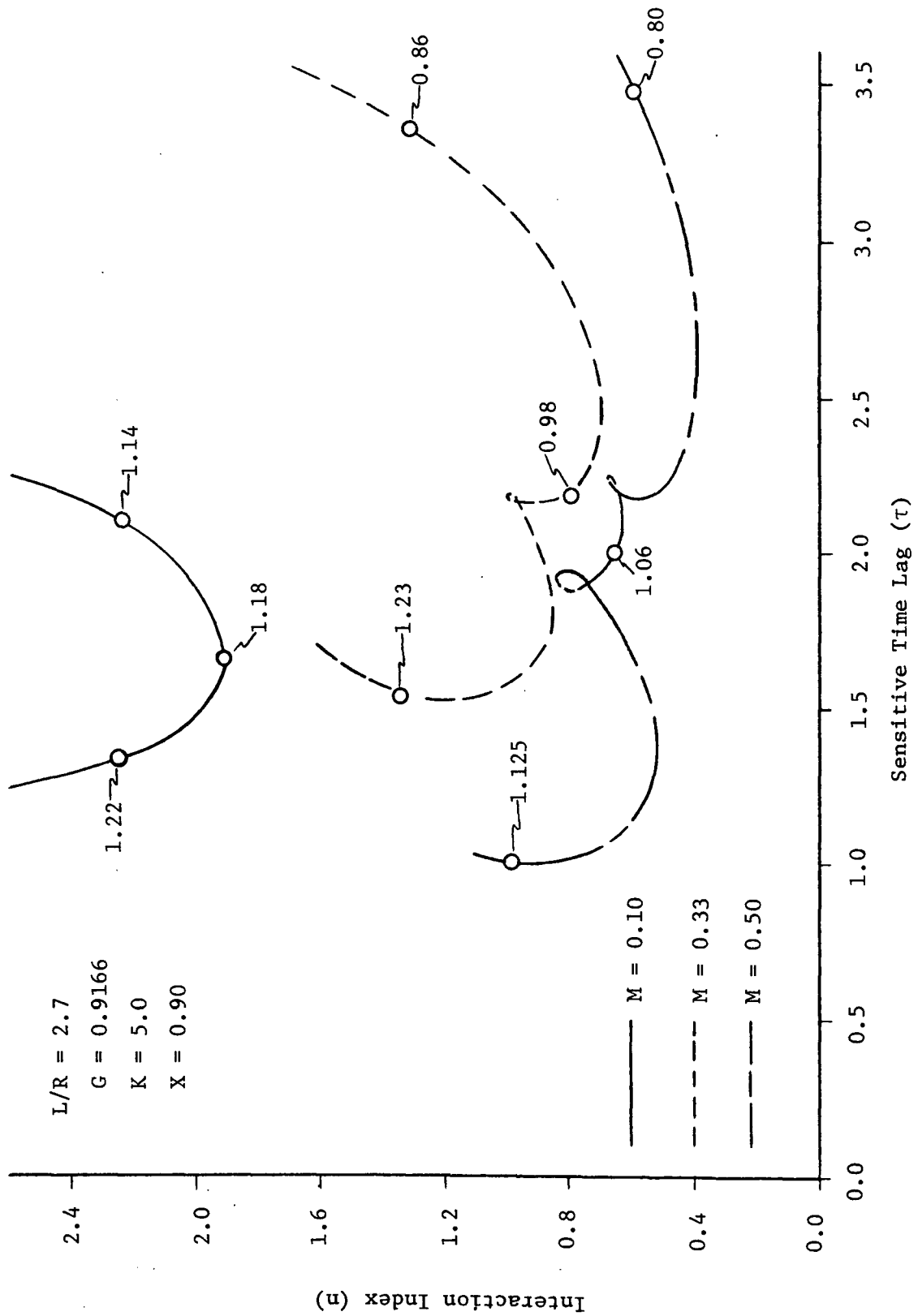


Figure 7 Effect of Mach Number on neutral stability - 1/3 length liner.

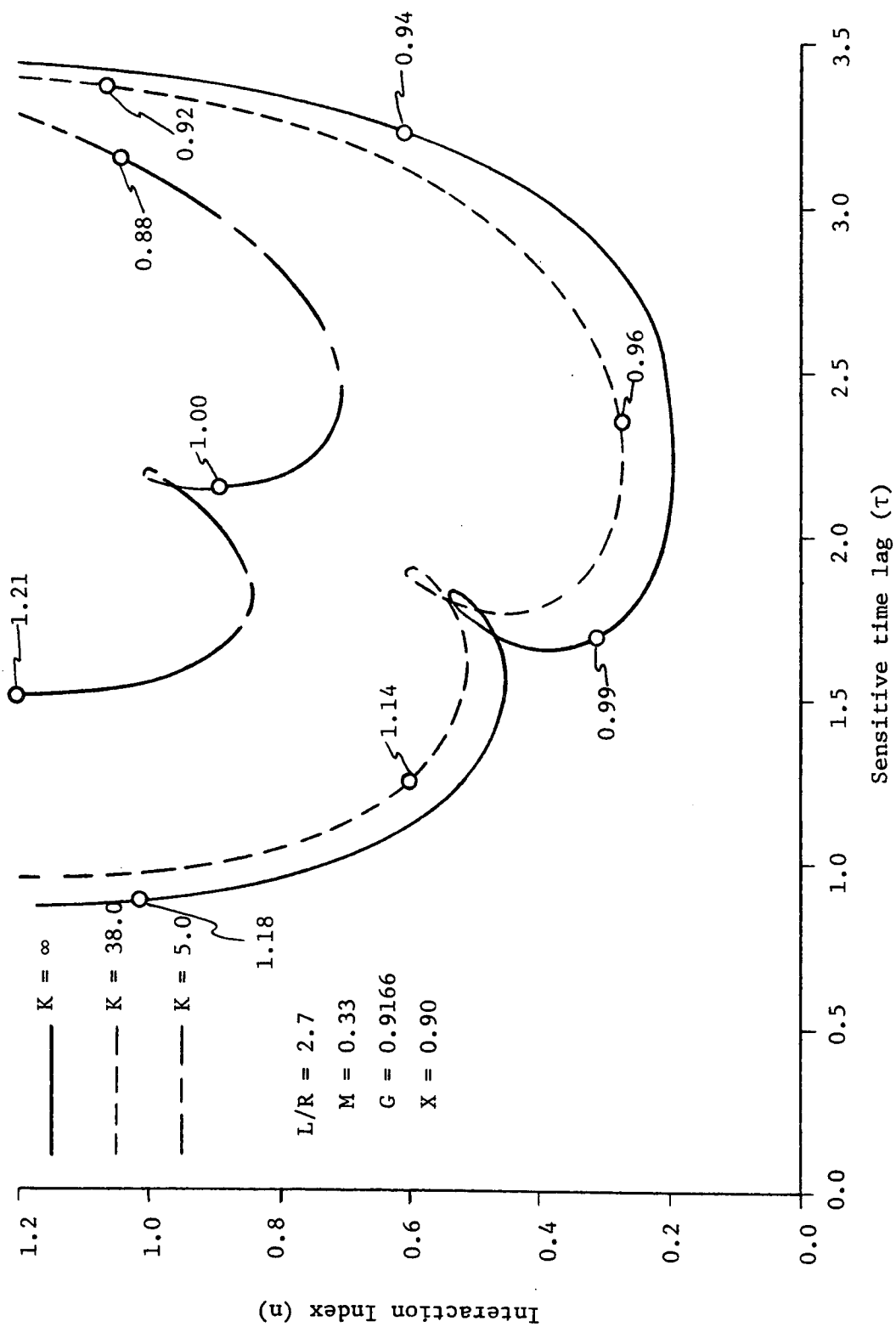
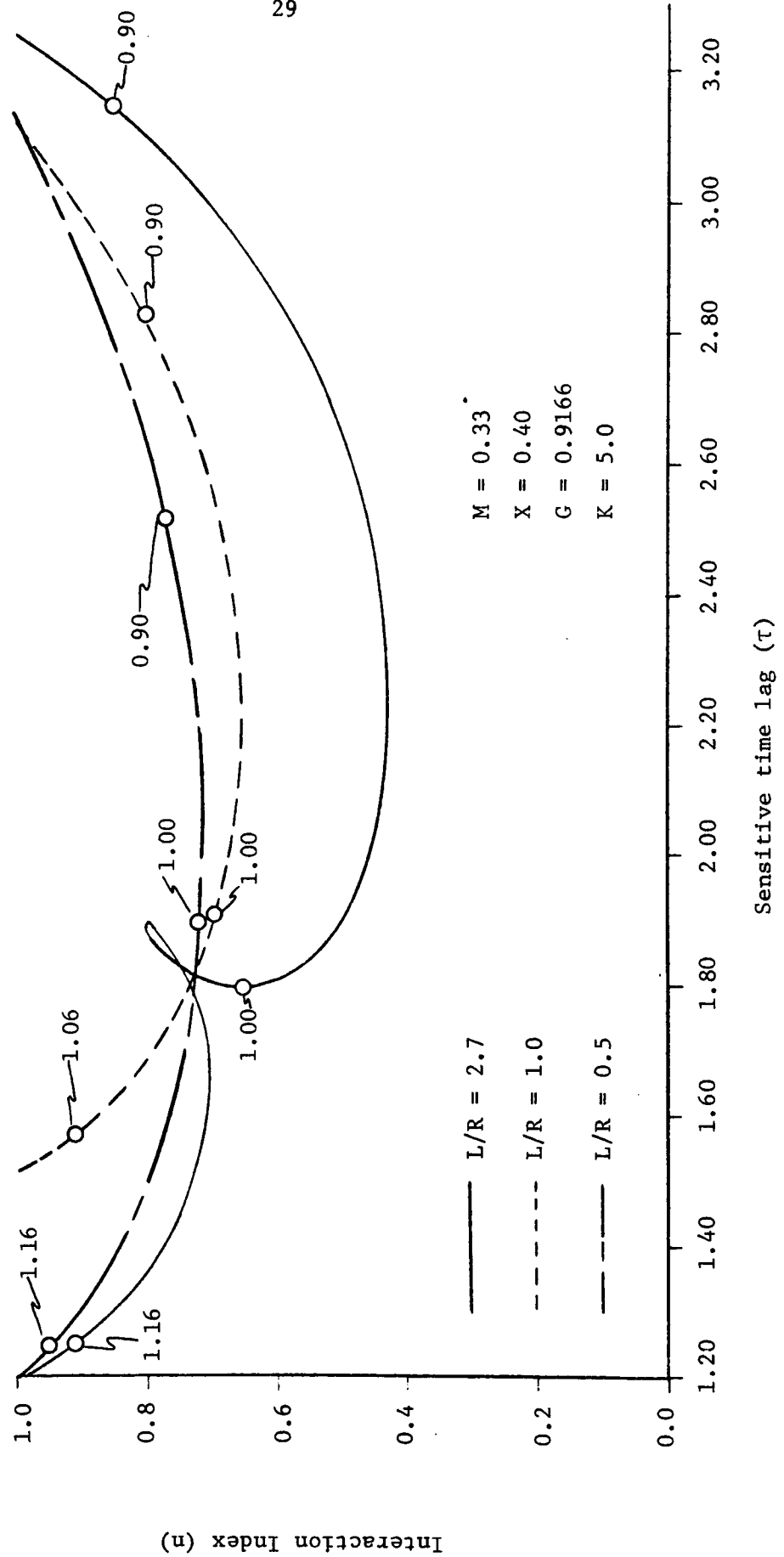


Figure 8 Effect of liner impedance - 1/3 length liner.

Figure 9 Effect of L/R

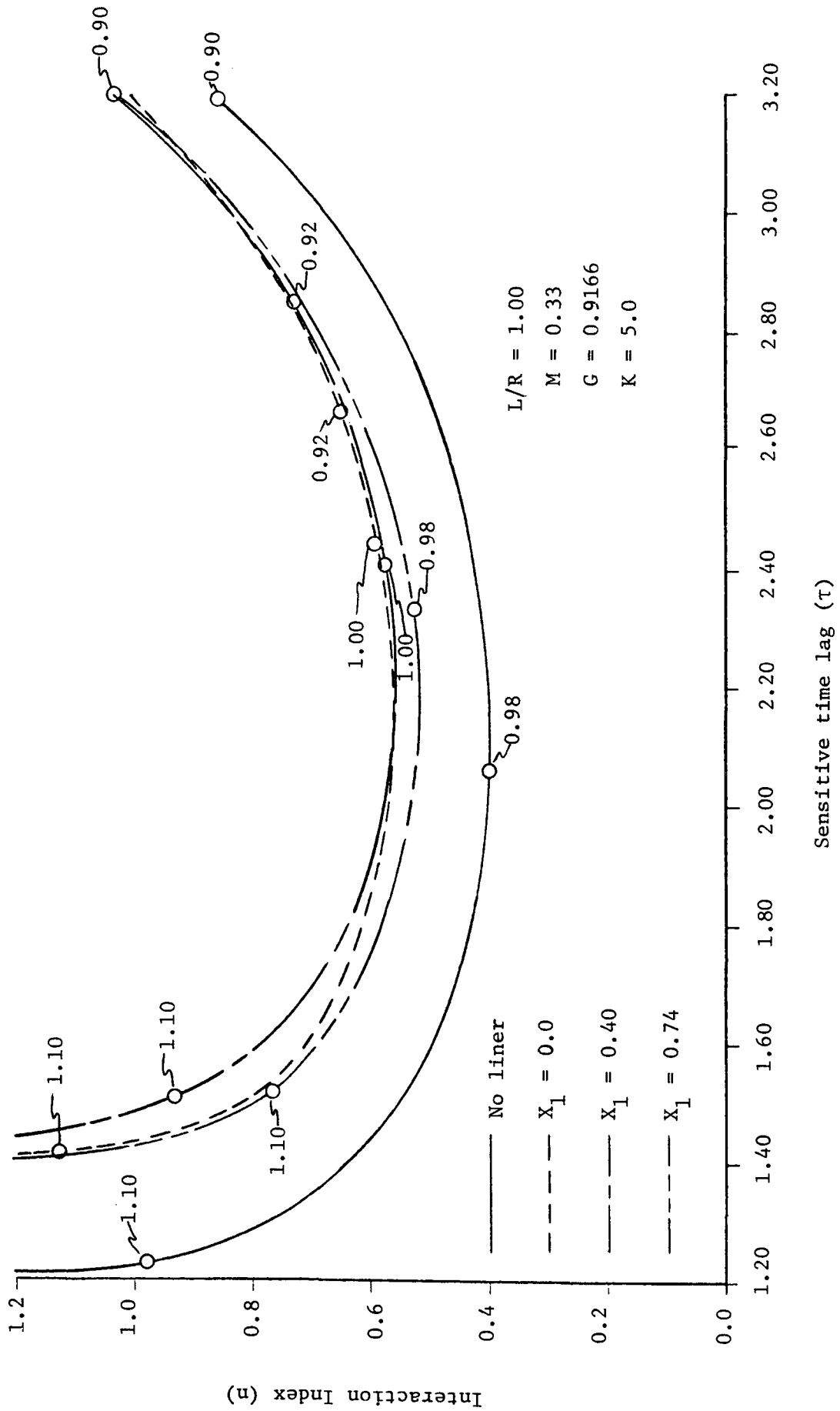


Figure 10 Effect of liner placement - 1/4 length liner.

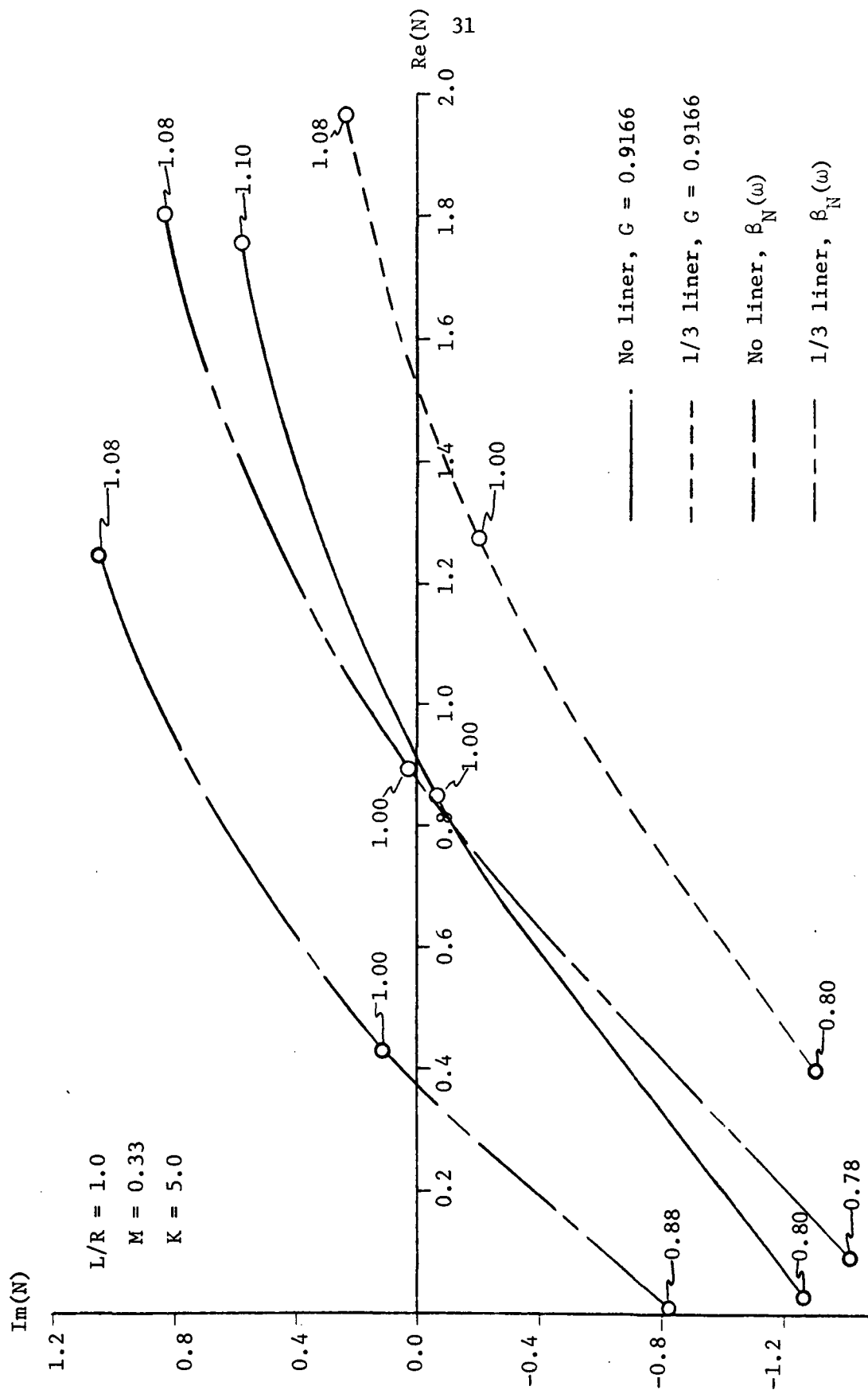


Figure 11 Effect of nozzle response.

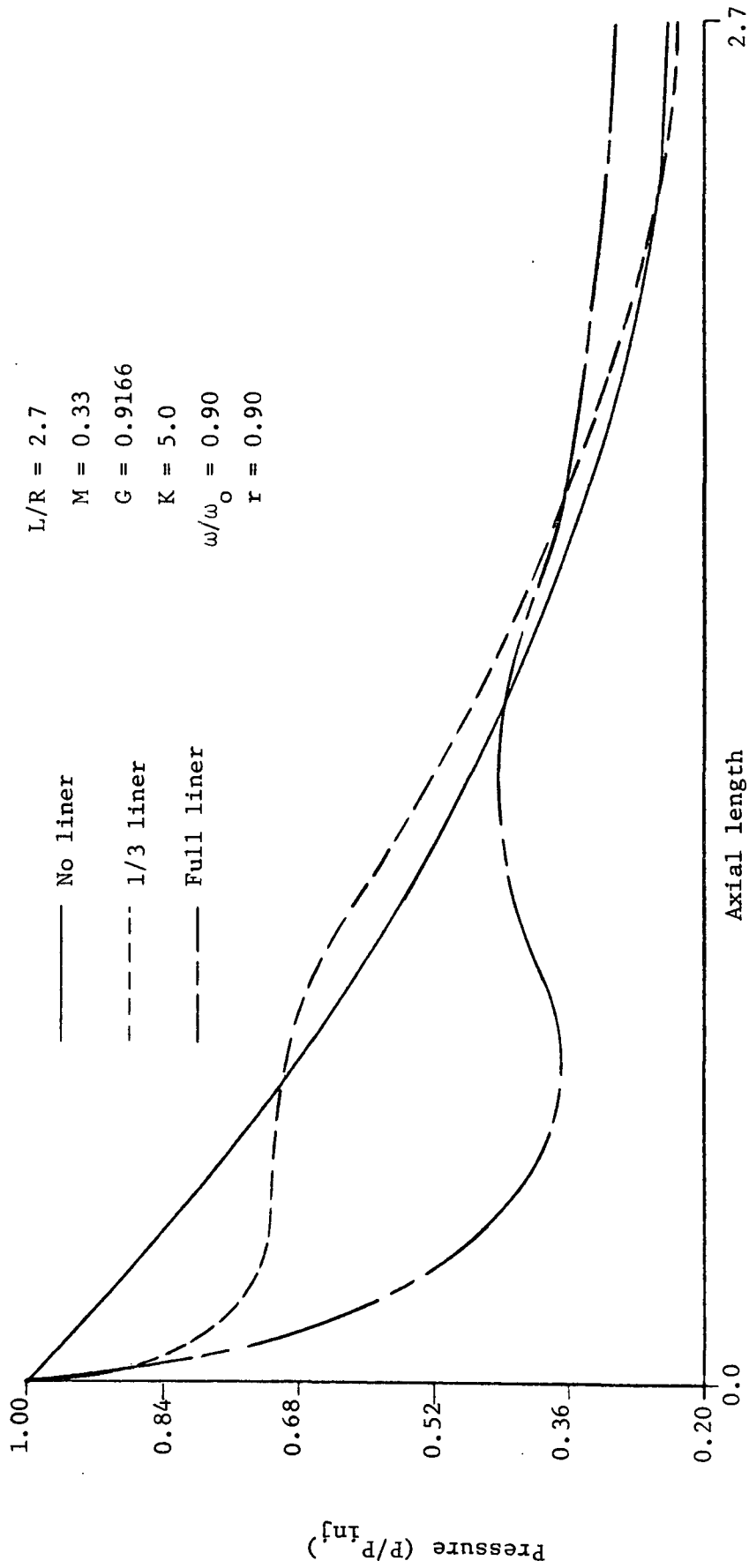


Figure 12 Pressure profiles for various length acoustic liners.

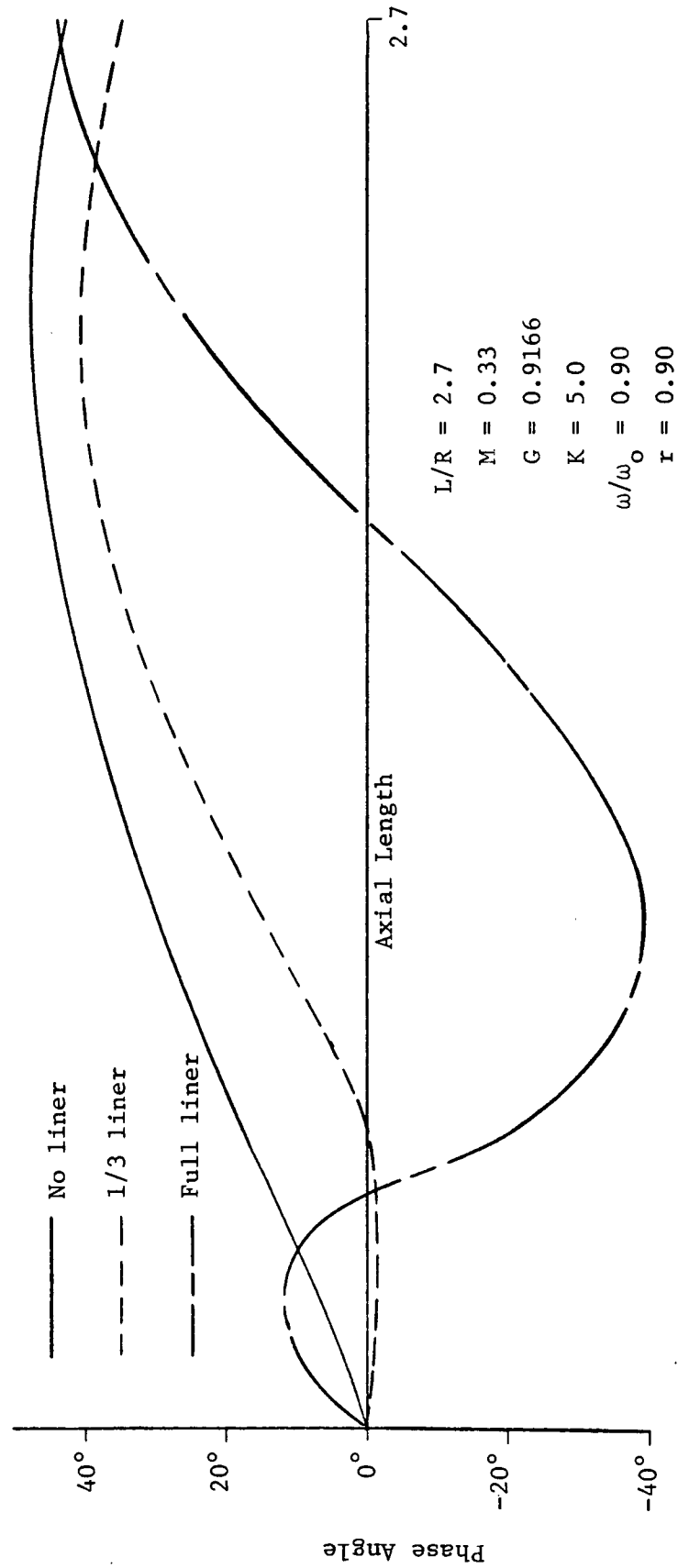


Figure 13 Phase angle profiles for various length acoustic liners.

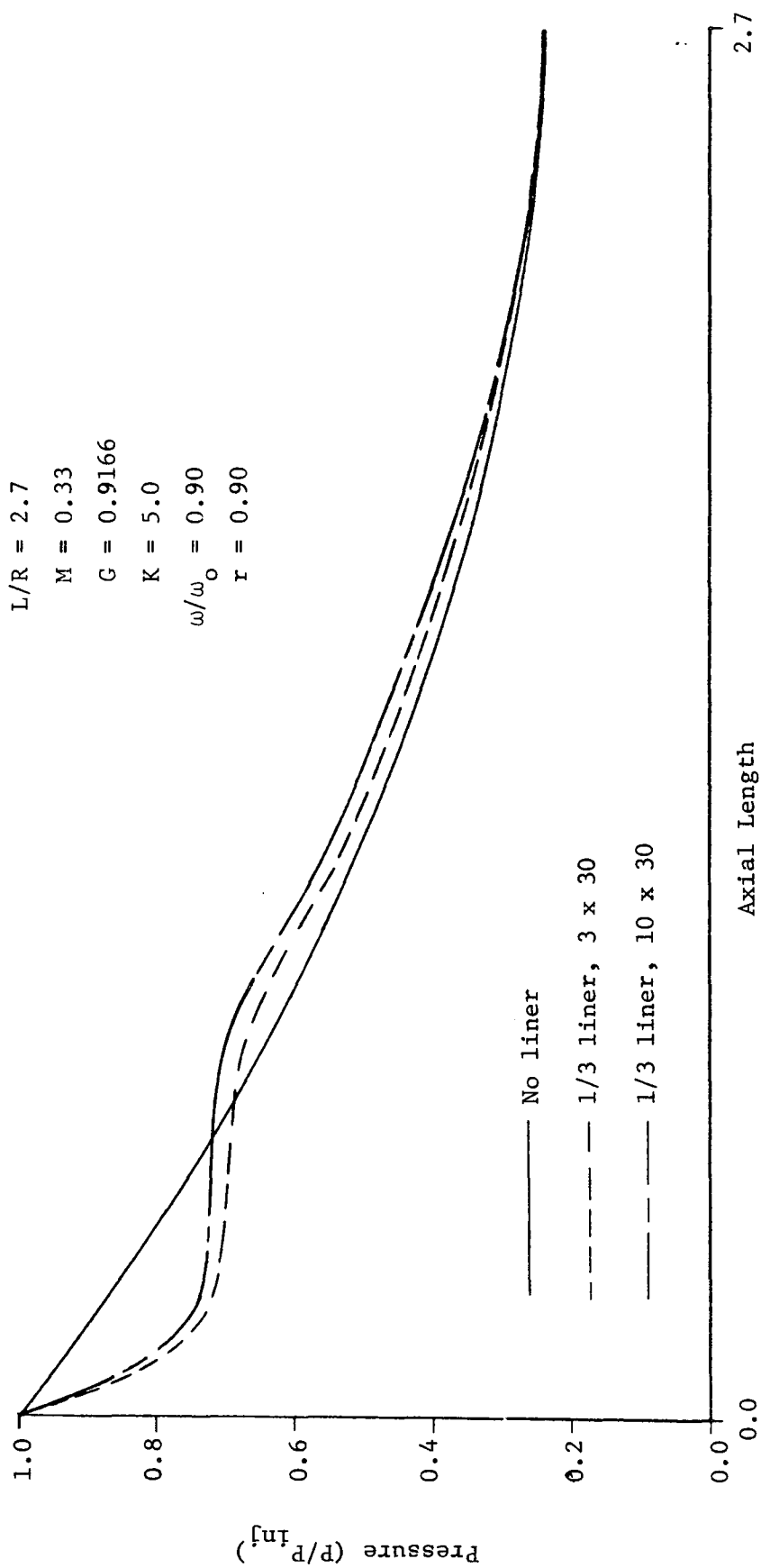


Figure 14 Comparison of small matrix and large matrix pressure profiles.

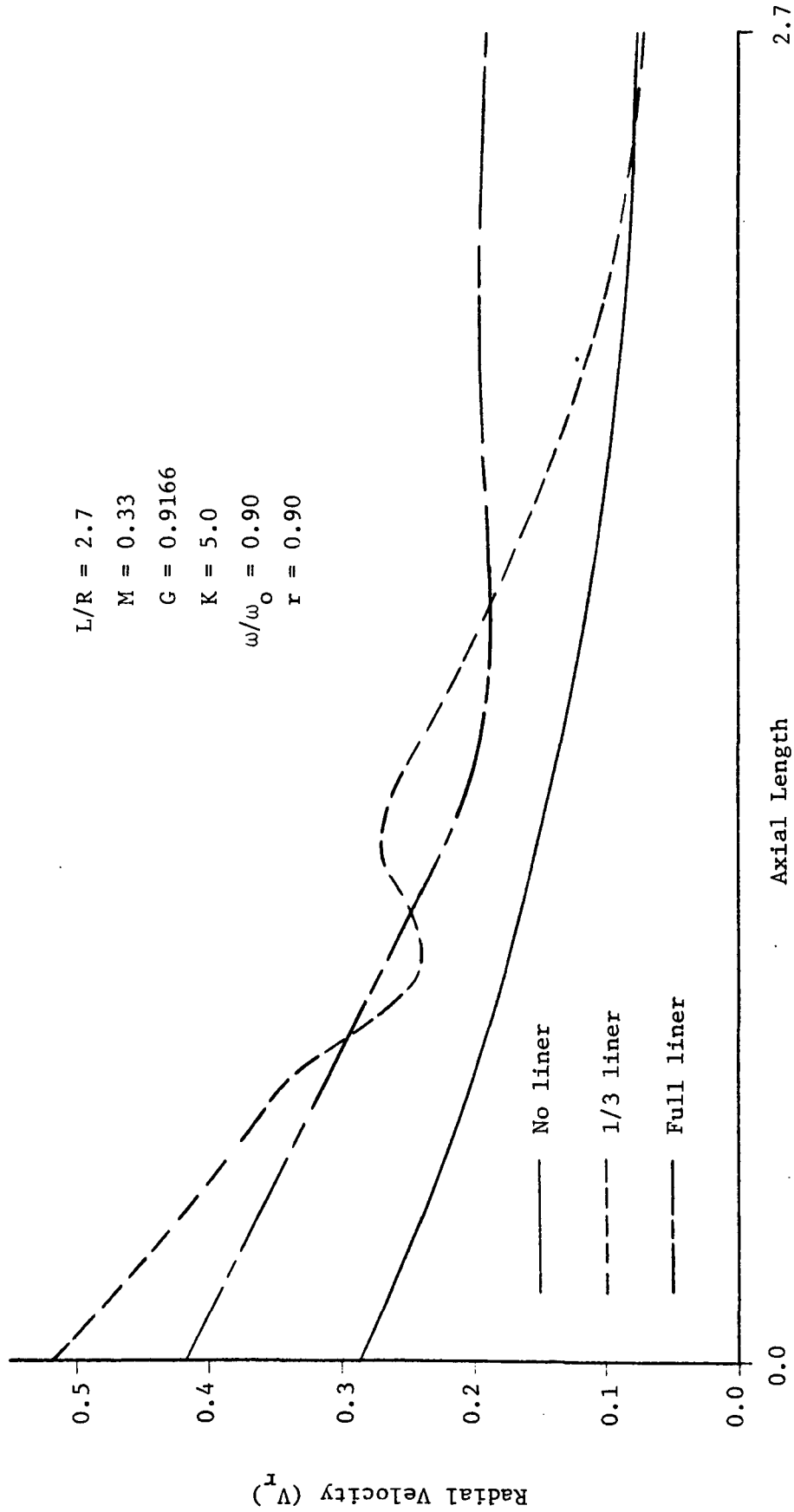


Figure 15 Radial velocity profiles for various length acoustic liners.

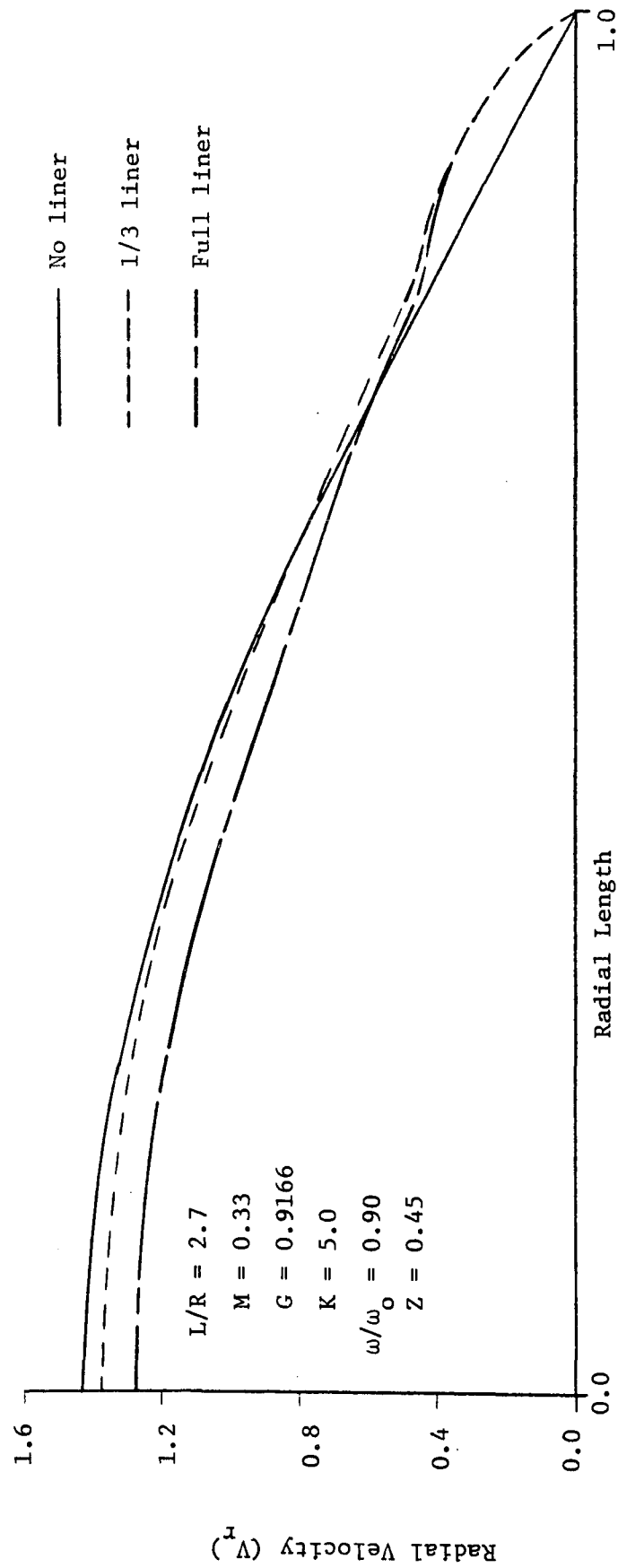


Figure 16 Radial velocity profiles for various length acoustic liners.

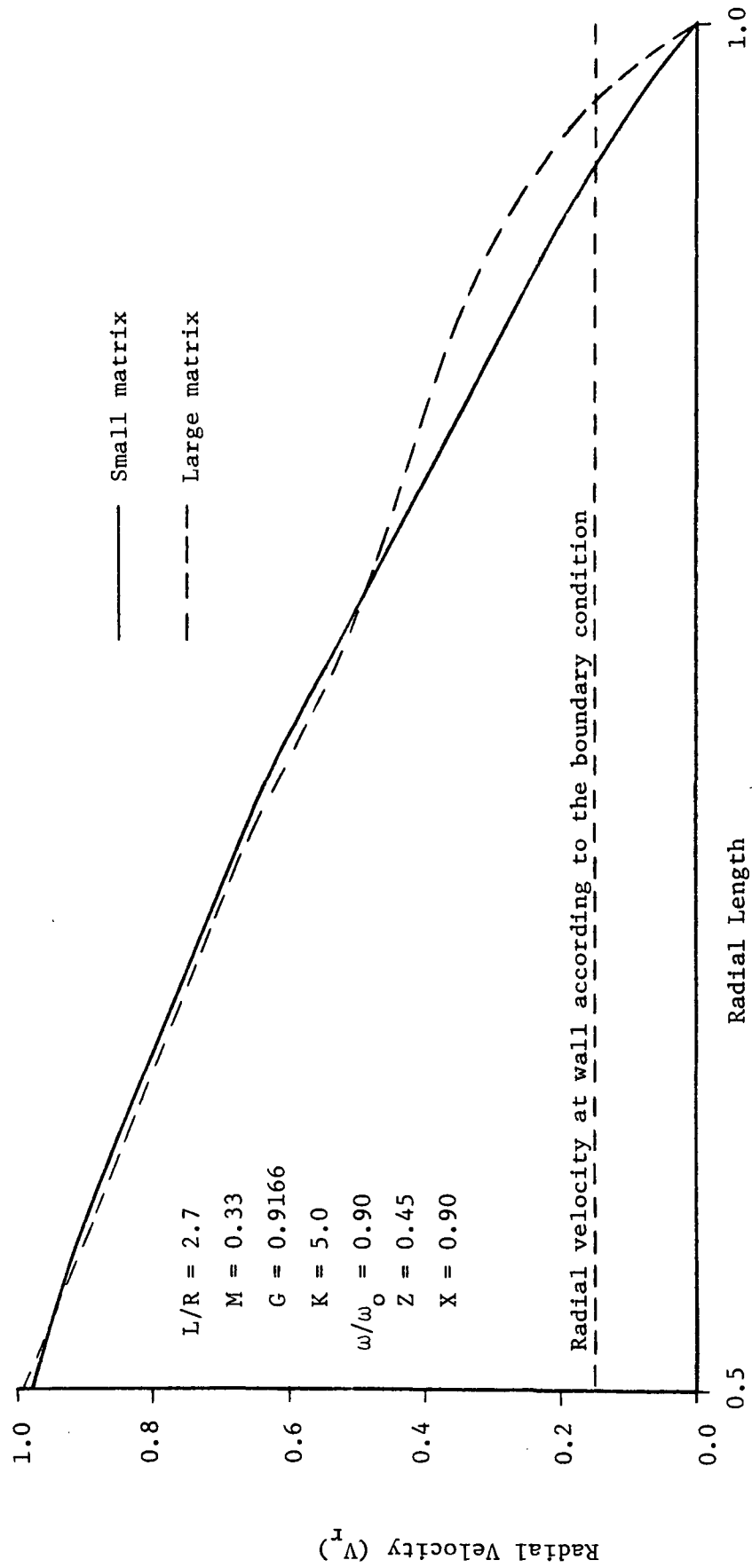


Figure 17 Radial velocity profiles for two different sizes of coefficient matrices.

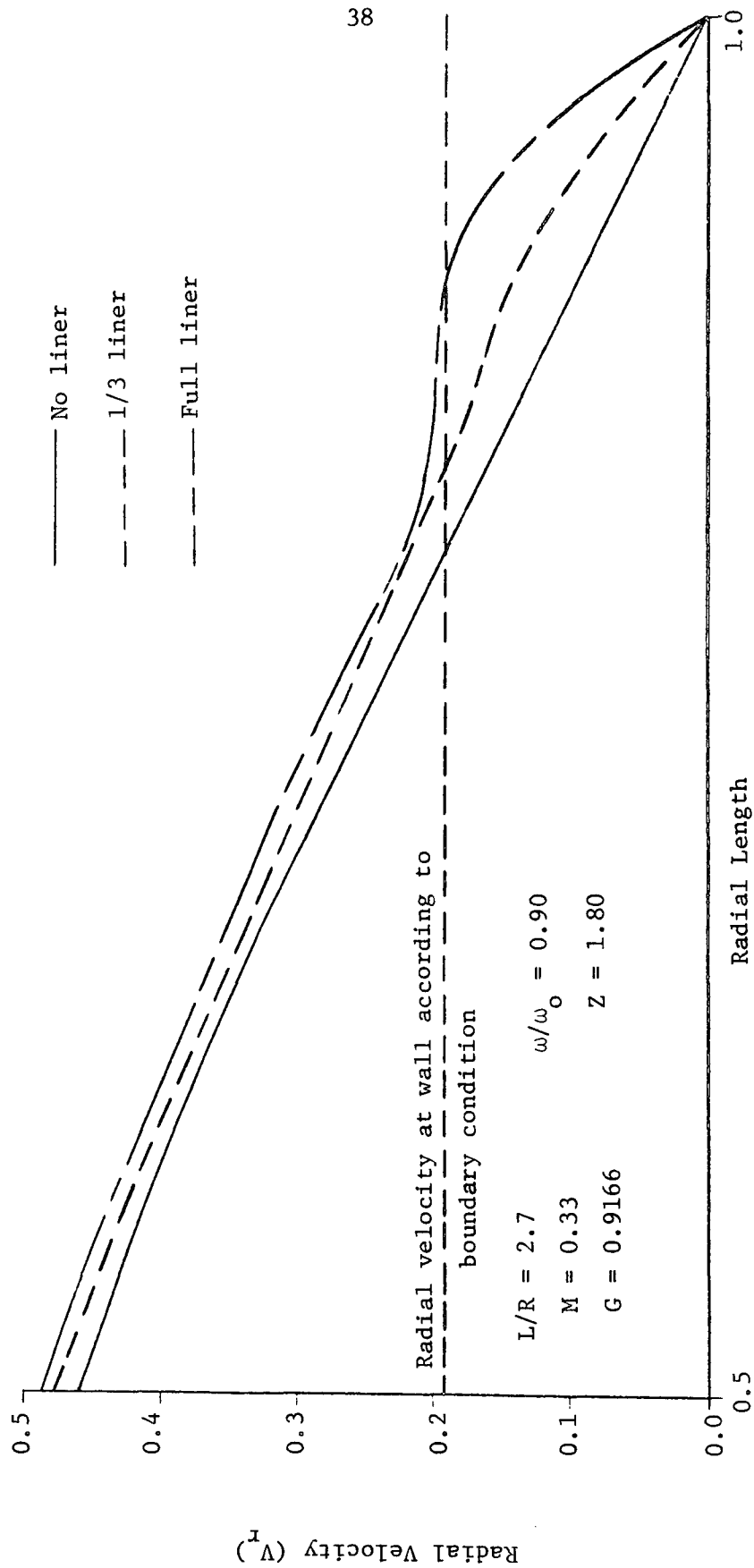


Figure 18 Radial velocity profile for various length acoustic liners, $Z = 1.80$

APPENDIX A

Basic Equations

The partial differential equation describing the chamber oscillations is

$$\nabla^2 \phi + \omega^2 \phi = M^2 \frac{\partial^2 \phi}{\partial z^2} + 2Mi\omega \frac{\partial \phi}{\partial z}$$

with the boundary condition $\nabla \phi \cdot \vec{n} = -\gamma\beta(i\omega\phi + M \frac{\partial \phi}{\partial z})$ on all surfaces. In order to convert this equation into an integral equation a Green's Function which satisfies the following equation is introduced

$$\nabla^2 G + \omega^2 G = \delta(\vec{r} - \vec{r}_0)$$

where $\nabla G \cdot \vec{n} = 0$ on all boundaries and δ is the usual delta function. The Green's Function is represented as an expansion in the orthonormal eigenfunctions for the chamber with no combustion or mean flow and solid walls as

$$G = \sum_{\ell} \sum_m \sum_n \frac{\Omega_{\ell mn}(\vec{r}) \Omega_{\ell mn}(\vec{r}_0)}{\omega^2 - \eta_{\ell mn}^2}$$

where $\Omega_{\ell mn}$ is one of the orthonormal eigenfunctions given by

$$\Omega_{\ell mn} = \cos m\theta J_m(\lambda_{\ell m} r) \cos \frac{n\pi z}{L} \cdot \frac{1}{\Lambda_{\ell mn}^{1/2}}$$

and

$$\eta_{\ell mn}^2 = \frac{n^2 \pi^2}{L^2} + \lambda_{\ell m}^2$$

The quantity $\lambda_{\ell m}^2$ is a root of the equation $\left[J'_m(\lambda_{\ell m} r) \right]_{r=1} = 0$ and $\Lambda_{\ell mn}$ is determined by the condition $\iiint_V \Omega_{\ell mn}^2 dV = 1$

The modified Green's Function, G_N , which appears in the integral

Equations (3) and (4) is just the Green's Function with one term in the series removed. That is, the term with $\ell = \hat{\ell}$, $m = \hat{m}$, and $n = \hat{n}$ (where $\hat{\ell}$, \hat{m} and \hat{n} are arbitrary) is deleted from the series for G_N . Thus

$$G_N = \sum_{\ell} \sum_m \sum_n \frac{\Omega_{\ell mn}(\vec{r}) \Omega_{\ell mn}(\vec{r}_0)}{\omega^2 - \eta_{\ell mn}^2} (1 - \delta(\ell, \hat{\ell}) \delta(m, \hat{m}) \delta(n, \hat{n}))$$

where $\delta(i, j) = 1$ if $i = j$ and $\delta(i, j) = 0$ if $i \neq j$.

In Equation (2) the quantity Ω_N can be interpreted as $\Omega_{\hat{\ell}\hat{m}\hat{n}}$ and in Equation (3) η_N is equivalent to $\eta_{\hat{\ell}\hat{m}\hat{n}}$. In the solution of Equations (2) and (3) the velocity potential and combustion response for the chamber with no liner but with mean flow are used as first approximations for ϕ and β_i . These quantities are called respectively $\tilde{\phi}$ and $\tilde{\beta}_i$. The form of $\tilde{\phi}$ can be found using the technique of separation of variables and is given by

$$\tilde{\phi} = \frac{\cos \hat{m}\theta}{\Lambda_{\hat{\ell}\hat{m}\hat{n}}^{1/2} \psi} J_{\hat{m}}(\lambda_{\hat{\ell}\hat{m}} r) (e^{izB_1} + C e^{izB_2})$$

where

$$B_1 = \frac{\omega M + [\omega^2 M^2 + (M^2 - 1)(\lambda_{\hat{\ell}\hat{m}}^2 - \omega^2)]^{1/2}}{(1 - M^2)}$$

$$B_2 = \frac{\omega M - [\omega^2 M^2 + (M^2 - 1)(\lambda_{\hat{\ell}\hat{m}}^2 - \omega^2)]^{1/2}}{(1 - M^2)}$$

$$C = - \frac{e^{iLB_1}}{e^{iLB_2}} \frac{[B_1 + \beta_N(\gamma\omega + \gamma MB_1)]}{[B_2 + \beta_N(\gamma\omega + \gamma MB_2)]}$$

and ψ is determined by the condition

$$\iiint_V \tilde{\phi} \Omega_{\ell mn} dv = 1.$$

$\tilde{\beta}_i$ is then determined from the boundary condition at the injector,

$$\nabla \tilde{\phi} \cdot \vec{n} = \tilde{\beta}_i \tilde{p}', \quad \text{or}$$

$$\beta_i = \frac{\frac{\partial \tilde{\phi}}{\partial z}}{(\gamma i \omega \tilde{\phi} + \gamma M \frac{\partial \phi}{\partial z})}$$

Substitution of $\tilde{\phi}$ and $\tilde{\beta}_i$ into Equations (2) and (3) as the initial step in the iteration procedure described earlier eventually leads to the following two relationships for the calculation of the j^{th} approximations for ϕ and β_i

$$\phi^{(j)} = \tilde{\phi} + \cos \hat{m}\theta \sum_{\ell} \sum_n \mu_{\ell n}^{(j)} J_{\hat{m}}(\lambda_{\ell \hat{m}} r) \cos \frac{n\pi z}{L}$$

$$\beta_i^{(j+1)} = \frac{\tilde{\beta}_i \int_{s_L} \Omega_N f_2(\tilde{\phi}) ds - \beta_N \int_{s_N} \Omega_N f_2(\phi^{(j)} - \tilde{\phi}) ds - M \int_V \Omega_N f_1(\phi^{(j)} - \phi) dV - \int_{s_c} \beta_c \Omega_N f_2(\phi^{(j)}) ds}{\int_{s_i} \Omega_N f_2(\phi^{(j)}) ds}$$

where $\mu_{\ell n}^{(j)}$ is a matrix dependent only upon $\phi^{(j-1)}$ and $\beta_i^{(j)}$ ($\mu_{\ell n}^{(1)}$ depends on $\tilde{\phi}$ and $\beta_i^{(1)}$; $\beta_i^{(1)}$ depends on $\tilde{\phi}$ and $\tilde{\beta}_i$), $f_2(y) = \gamma i \omega y + M \frac{\partial y}{\partial z}$, $f_1(y) = 2i\omega \frac{\partial y}{\partial z} + M \frac{\partial^2 y}{\partial z^2}$, s_i is the surface of the injector, s_N is the surface of the nozzle exit plane, s_c is the surface of the liner and V is the chamber volume. For any solution, values of $\hat{\ell}$, \hat{m} , and \hat{n} must be selected. These integers will determine the general acoustic waveform of ϕ expected and the exact waveform for $\tilde{\phi}$. For example $\hat{m} = 1$, $\hat{\ell} = 1$, $\hat{n} = 0$ gives the solution for the pure first transverse mode. If the wrong values of \hat{m} , $\hat{\ell}$, \hat{n} are selected for a given frequency value the iteration technique will fail. That is, if the solution is a first

transverse mode type oscillation and a combined first transverse - second longitudinal mode is assumed (by taking $\hat{m} = 1$, $\hat{\ell} = 1$, $\hat{n} = 2$) the iteration scheme will not work until the value of \hat{n} is changed to $\hat{n} = 0$.

APPENDIX B

Computer Program

This section describes the use of the computer program, COMBADM, for the determination of the neutral stability curves for a given set of input parameters which characterize the combustion chamber. The program was written in FORTRAN IV to run on a CDC 6400. Very little effort was made to optimize the program with respect to running time.

The program, COMBADM, calculates two neutral stability curves for a given combustor as a function of frequency. The first combustion admittance calculated for each frequency is the neutral stability point for the combustor with no liner. This point corresponds to BETAWI in the output. The last value of the combustion admittance listed for each frequency is for the combustor with the acoustic liner. This point is determined by the method of successive approximations. The first approximation to the combustion admittance for the lined chamber is that of the unlined combustor. The combustion admittance is then used to calculate a velocity potential for the lined combustor and then a new admittance is calculated for the combustor. This technique proceeds until the error between successive iterations is within pre-determined limits. The accuracy of the combustion admittance calculated is limited only by the size of the coefficient matrix used in the calculation of the velocity potential.

The input parameters are:

1. LENGNO - the problem identifier
2. F - the initial frequency ratio of the combustor
3. ALENGTH - the length to radius ratio for the combustor

4. AMACH - mean flow Mach Number
5. GAMMA - ratio of specific heats
6. G - complex number specifying the acoustic impedance of the nozzle
7. AK - complex number specifying the acoustic impedance of the liner
8. X1 - the beginning of the liner opening with respect to the injector
9. X2 - the end of the liner opening with respect to the injector
10. ERROR1 - the maximum acceptable error in the real part of the combustion admittance
11. ERROR2 - the maximum acceptable error in the imaginary part of the combustion admittance
12. LHAT - radial acoustic mode number
13. MHAT - transverse acoustic mode number
14. NHAT - longitudinal acoustic mode number
15. LDEX - specifies the number of radial terms in the coefficient matrix
16. NDEX - specifies the number of longitudinal terms in the coefficient matrix
17. MATRIX - identifier used to determine whether or not the coefficient matrix is printed out
18. FINC - the increment size of the frequency ratio

19. FMAX - the maximum frequency for which a combustion admittance is calculated

The output from the program lists the input variables, the combustion admittance and the combustion impedance.

Sample Calculation

An example of the output from COMBADM is shown on the page immediately following the listing of the program. The example shown is typical of many cases that can be run. In the output the neutral stability point for the unlined combustor is denoted as BETAWI and the neutral stability point for the lined combustor to the specified accuracy is the last two numerical values listed, where the first of these values, BETAI(J), is the combustion admittance and the latter value, N, is the combustion impedance. The only problem likely to be encountered in the program is the selection of the appropriate longitudinal acoustic mode (NHAT), i.e., as the frequency increases higher order longitudinal modes are more dominant in the solution and NHAT often must be increased from zero to one or even two in order for the iteration process to converge. (See Appendix A)

The form of the input for COMBADM is shown immediately following the list of the program. The input is on three data cards as follows:

Card 1

Columns	Variable	Type
1-10	LENGNO	Alphanumeric word
11-20	Re(F)	Real number
21-30	Im(F)	Real number

B-4

Columns	Variable	Type
31-40	ALENGTH	Real number
41-50	AMACH	Real number
51-60	GAMMA	Real number
61-70	Re(G)	Real number
71-80	Im(G)	Real number

Card 2

Columns	Variable	Type
1-10	Re(AK)	Real number
11-20	Im(AK)	Real number
21-30	X1	Real number
31-40	X2	Real number
41-50	ERROR1	Real number
51-60	ERROR2	Real number
61-63	LHAT	Integer
64-66	MHAT	Integer
67-69	NHAT	Integer
70-72	LDEX	Integer
73-75	NDEX	Integer
76-80	MATRIX*	Alphanumeric word

*If the coefficient matrix is to be printed out, then MATRIX is printed as YESBB, where B signifies a blank.

Card 3

Columns	Variable	Type
1-10	Re(FINC)	Real number
11-20	Im(FINC)	Real number
21-30	Re(FMAX)	Real number
31-40	Im(FMAX)	Real number

The last page is the output and includes the essential input variables and the two neutral stability points.

NomenclatureCOMBADM

ω	OMEGA
M	AMACH
γ	GAMMA
η	Function ETA
$J'_m(\lambda_{\ell m})$	Function BESPRIM
$J_m(\lambda_{\ell m})$	Function BESSEL
$\Lambda_{\ell mn}^{1/2}$	Function FNORM
Ψ	Function PSI
B_1	BETA1
B_2	BETA2
C	C
$\tilde{\beta}_i$	BETAWI
β_i	BETAI or TETAIS
β_c	BETAC
β_N	BETAN
$\mu_{\ell n}$	AMU

```

PROGRAM COMBADM(OUTPUT=101,TAPE6=OUTPUT,INPUT=101,TAPE5=INPUT)
COMPLEX BETA1, BETA2, BETAN, BETAC, BETA1, BETAW1, OMEGA, C, AK1,
1 AK2, PSI2, AMU, BETAIS, C12
COMPLEX G, AN, AK, A, A4, A5, BETA, DUM1, DUM2, PSI, DUMMY, G1,
1 G2, F, AKA, FINC, FMAX
COMMON / BLKA / BETA1, BETA2, AMACH, GAMMA, OMEGA, ALENGTH, C, AK1
1, AK2, BETAN, RLMDA, BETA1, BETAC, BETAW1, LHAT, MHAT, NHAT,
1 PSI2, X1, X2/BLKB/AMU(10,30,29),BETAIS(30),A
COMMON C12(30,30), ISET, LDEX, NDEX, ERROR1, ERROR2
2 READ(5,200) LENGNO, F, ALENGTH, AMACH, GAMMA, G, AK, X1, X2, ERROR1, ERROR2,
1 LHAT, MHAT, NHAT, LDEX, NDEX, MATRIX, FINC, FMAX
IF ( EOF , 5 ) 50 , 3
3 A = CMPLX ( 1.0 , 0.0 )
RLMDA = BESPRIM ( MHAT + 1 , LHAT )
7 CONTINUE
NHA1 = NHAT + 1
OMEGA=F*1.84118378
BETAC = 1./GAMMA/AK
BETAN = AMACH * ( G - 1. / GAMMA )
BETA=CSQRT(OMEGA*AMACH*OMEGA*AMACH+(AMACH*AMACH-1.)*(RLMDA**2 -
1 OMEGA*OMEGA))/(1.-AMACH*AMACH)
BETA1=(OMEGA*AMACH)/(1.-AMACH*AMACH)+BETA
BETA2=(BETA1)-2.*BETA
A4 = CMPLX( -AIMAG(BETA1), REAL(BETA1))
DUM1 = CMPLX( -AIMAG(BETA2), REAL(BETA2))
C = - CEXP(ALENGTH*A4) / CEXP(ALENGTH*DUM1)
C = C * (BETA1 + BETAN * GAMMA * (OMEGA + AMACH * BETA1)) / (
1 BETA2 + BETAN * GAMMA * (OMEGA + AMACH * BETA2))
PSI2 = PSI( DUMMY )**2
AK1=(OMEGA+ AMACH *BETA1+C*(OMEGA+ AMACH*BETA2))*GAMMA
AK1= CMPLX(-AIMAG(AK1),REAL(AK1))
DUM1 = CMPLX(-AIMAG(BETA1),REAL(BETA1))
DUM1 = DUM1*ALENGTH
DUM2 = CMPLX(-AIMAG(BETA2),REAL(BETA2))
DUM2 = DUM2*ALENGTH
AK2 = ((OMEGA+AMACH*BETA1)*CEXP(DUM1)+(OMEGA+AMACH*BETA2)*C*CEXP(
1 DUM2))*GAMMA
AK2 = CMPLX(-AIMAG(AK2),REAL(AK2))
CALL CALCA4( A4, A5 )
BETAW1 = (OMEGA**2 - ETA(LHAT,MHAT,NHA1,ALENGTH,RLMDA)-(AMACH*G2(
1 MHAT)/EPSIZN(LHAT,MHAT,NHAT,ALENGTH,RLMDA)+BETAN*AK2/EPSIZN(LHAT,
1 MHAT,NHAT,ALENGTH,RLMDA)*(-1.))**(NHAT+2))/PSI(DUMMY))/A4
BETA1 = BETAW1 - A5 / A4

```

```

BETAIS(1)=BETA1
WRITE(6,100) LENGNO
WRITE(6,110) LDEX , NDEX
WRITE(6,116) AMACH
WRITE(6,117) GAMMA
WRITE(6,118) OMEGA
WRITE(6,119) ALENGTH
WRITE(6,101) LHAT, MHAT, NHAT
WRITE(6,115) X1,X2
WRITE(6,113) F
WRITE(6,114) A
WRITE(6,102) BETAN
WRITE(6,120) G
WRITE(6,121) BETAC
WRITE(6,108) AK
WRITE(6,105) BETAWI
AN = 1. / GAMMA - BETAWI / AMACH
WRITE(6,103) AN
BETAWI = ( BETA1 + C * BETA2 ) / ( GAMMA * ( OMEGA * ( 1. + C ) +
1 AMACH * ( BETA1 + C * BETA2 ) ) )
WRITE(6,112) BETAWI
AN = 1. / GAMMA - BETAWI / AMACH
WRITE(6,103) AN
WRITE(6,109) BETAIS(1)
AN = 1. / GAMMA - BETAIS(1) / AMACH
WRITE(6,103) AN
JX = 30
JY = JX - 1
CALL CALMU( JY )
JX = JY + 1
IF ( MATRIX .NE. 3HYES ) GO TO 1
DO 6 J = 1, JY
KS = 1
KF = 3
WRITE(6,106) J, KS, KF
DO 6 L=1,30
6 WRITE(6,104) L, ( AMU(I,L,J), I = KS, KF )
1 CONTINUE
F = F + FJNC
IF ( JX .EQ. 30 .OR. F .GT. FMAX ) 2, 7
50 CALL EXIT
100 FORMAT('1 THIS IS ENGINE NUMBER 'A10)
101 FORMAT('0 THE PRIMARY MODE ASSUMED IS LHAT = ',12,' MHAT = ',12,

```

```

      INHAT = ',12)
102 FORMAT('O BETAN = ',2G21.14)
103 FORMAT('+',70X,' N = ',2G21.14,'1')
104 FORMAT(' ',13,' ',10G13.6)
105 FORMAT('O BETAWI = ',2G21.14)
106 FORMAT('O N          J EQUAL ',12,'          L EQUAL ',11,' TO ',12)
107 FORMAT('O ',G21.14,' WAS THE TIME FOR THE ITERATION ',G21.14)
108 FORMAT('+',70X,' K = ',2G21.14)
109 FORMAT('O BETA(1) = ',2G21.14)
110 FORMAT('+',70X,' THE COEFFICIENT MATRIX IS ',12,' X ',13)
112 FORMAT('O BETAWID = ',2G21.14)
113 FORMAT('O W/WO = ',2G21.14)
114 FORMAT('+',70X,' A = ',2G21.14)
115 FORMAT('+',70X,' THE LINER BEGINS AT ',F6.4,' AND ENDS AT ',F6.4)
116 FORMAT('O THE MACH NUMBER IS ',G21.14)
117 FORMAT('+',70X,' THE RATIO OF SPECIFIC HEATS IS ',G21.14)
118 FORMAT('O THE FREQUENCY IS ',2G21.14)
119 FORMAT('+',70X,' THE LENGTH OF THE COMBUSTOR IS ',G21.14)
120 FORMAT('+',70X,' G = ',2G21.14)
121 FORMAT('O BETAC = ',2G21.14)
200 FORMAT(A10,7F10.0/6F10.0,5I3,A5/4F10.0)
      END
      FUNCTION BESPRIM (M, L)
      DIMENSION A(10,5)
C**** THESE ARE THE ROOTS OF THE DERIVATIVE OF THE BESSEL FUNCTION OF ORDER ZEO
C**** SET EQUAL TO ZERO
      A(1,1) = 0.00000000
      A(2,1) = 3.83170597
      A(3,1) = 7.01558667
      A(4,1) = 10.17346814
      A(5,1) = 13.32369194
      A(6,1) = 16.47063005
      A(7,1) = 19.61585851
      A(8,1) = 22.76008438
      A(9,1) = 25.90367209
      A(10,1) = 29.04682853
C**** THESE ARE THE ROOTS OF THE DERIVATIVE OF THE BESSEL FUNCTION OF ORDER ON
C**** SET EQUAL TO ZERO
      A(1,2) = 1.84118378
      A(2,2) = 5.33144277
      A(3,2) = 8.53631637
      A(4,2) = 11.70600490
      A(5,2) = 14.86358863

```

```

A(6 ,2) = 18.01552786
A(7 ,2) = 21.16436986
A(8 ,2) = 24.31132686
A(9 ,2) = 27.45705057
A(10,2) = 30.60192297
C**** THESE ARE THE ROOTS OF THE DERIVATIVE OF THE BESSEL FUNCTION OF ORDER TW
C**** SET EQUAL TO ZERO
A(1 ,3) = 3.05423693
A(2 ,3) = 6.70613319
A(3 ,3) = 9.96946782
A(4 ,3) = 13.17037086
A(5 ,3) = 16.34752232
A(6 ,3) = 19.51291278
A(7 ,3) = 22.67158177
A(8 ,3) = 25.82603714
A(9 ,3) = 28.97767277
A(10,3) = 32.12732702
C**** THESE ARE THE ROOTS OF THE DERIVATIVE OF THE BESSEL FUNCTION OF ORDER 3
C**** SET EQUAL TO ZERO
A(1 ,4) = 4.20118894
A(2 ,4) = 8.01523660
A(3 ,4) = 11.34592431
A(4 ,4) = 14.58584829
A(5 ,4) = 17.78874787
A(6 ,4) = 20.97247694
A(7 ,4) = 24.14489743
A(8 ,4) = 27.31005793
A(9 ,4) = 30.47026881
A(10,4) = 33.62694918
C**** THESE ARE THE ROOTS OF THE DERIVATIVE OF THE BESSEL FUNCTION OF ORDER FOR
C**** SET EQUAL TO ZERO
A(1 ,5) = 5.31755313
A(2 ,5) = 9.28239629
A(3 ,5) = 12.68190844
A(4 ,5) = 15.96410704
A(5 ,5) = 19.19602880
A(6 ,5) = 22.40103227
A(7 ,5) = 25.58975968
A(8 ,5) = 28.76783622
A(9 ,5) = 31.93853934
A(10,5) = 35.10391668
1 BESPRIM = A(L, M)
RETURN

```

ENTRY BESSEL

C**** THESE ARE THE BESSEL NUMBERS OF ORDER ZERO FOR THE ZEROS OF THE BESSEL
C**** FUNCTION

A(1,1) = 1.00000000
A(2,1) = -0.4027588095
A(3,1) = 0.301128303
A(4,1) = -0.249704877
A(5,1) = 0.218359407
A(6,1) = -0.19645371
A(7,1) = 0.180063375
A(8,1) = -0.167184600
A(9,1) = 0.156724985
A(10,1) = -0.148011108

C**** THESE ARE THE BESSEL NUMBERS OF ORDER ONE FOR THE ZEROS OF THE BESSEL
C**** FUNCTION

A(1,2) = 0.5818649368
A(2,2) = -0.3461258542
A(3,2) = 0.2732981131
A(4,2) = -0.233304416
A(5,2) = 0.207012651
A(6,2) = -0.188017488
A(7,2) = 0.173459050
A(8,2) = -0.161838211
A(9,2) = 0.152282069
A(10,2) = -0.144242905

C**** THESE ARE THE BESSEL NUMBERS OF ORDER TWO FOR THE ZEROS OF THE BESSEL
C**** FUNCTION

A(1,3) = 0.4864961885
A(2,3) = -0.3135283099
A(3,3) = 0.2547441235
A(4,3) = -0.220881581
A(5,3) = 0.197937434
A(6,3) = -0.181010000
A(7,3) = 0.167835534
A(8,3) = -0.157195167
A(9,3) = 0.148363778
A(10,3) = -0.140878333

C**** THESE ARE THE BESSEL NUMBERS OF ORDER THREE FOR THE ZEROS OF THE BESSEL
C**** FUNCTION

A(1,4) = 0.4343942763
A(2,4) = -0.2911584413
A(3,4) = 0.240738175
A(4,4) = -0.210965204

```

A(5,4) = 0.190419022
A(6,4) = -0.175048405
A(7,4) = 0.162954965
A(8,4) = -0.153102409
A(9,4) = 0.144866574
A(10,4) = -0.137844513

```

```

C**** THESE ARE THE BESSEL NUMBERS OF ORDER FOUR FOR THE ZEROS OF THE BESSEL
C**** FUNCTION

```

```

A(1,5) = 0.3996514545
A(2,5) = -0.2743809949
A(3,5) = 0.229590468
A(4,5) = -0.202763849
A(5,5) = 0.184029896
A(6,5) = -0.169878516
A(7,5) = 0.158655372
A(8,5) = -0.149451156
A(9,5) = 0.141714307
A(10,5) = -0.135086328

```

```

GO TO 1

```

```

END

```

```

SUBROUTINE BETAIJ(J)

```

```

COMPLEX A150,A151,A152,A153,A155,A155J,DUM1,PSI,AMU,BETAIS,COMEGA,
1DUMMY,FNORM,A, C12,SUM1,SUM2,SUM3,SUM4, AN

```

```

COMPLEX BETA1, BETA2, BETAN, BETAC, BETA1, BETAWI, OMEGA, C, AK1,
1AK2, PSI2

```

```

COMMON / BLKA / BETA1, BETA2, AMACH, GAMMA, OMEGA, ALENGTH, C, AK1
1, AK2, BETAN, RLMDA, BETA1, BETAC, BETAWI, LHAT, MHAT, NHAT,
1PSI2,X1,X2/BLKB/AMU(10,30,29),BETAIS(30),A

```

```

COMMON C12(30,30), ISET, LDEX, NDEX, ERROR1, ERROR2

```

```

NHAT = NHAT + 1

```

```

COMEGA=CMPLX(-AIMAG(OMEGA),REAL(OMEGA))

```

```

SUM1=SUM2=SUM3=SUM4=CMPLX(0.0,0.0)

```

```

DO 10 LP = 1, LDEX

```

```

DUM =BESSEL(MHAT+1,LP)

```

```

DO 10 NP = 1, NDEX

```

```

SUM4=SUM4 + AMU(LP,NP,J-1)*DUM *C12(NHAT+1,NP)

```

```

10 CONTINUE

```

```

DO 20 NP = 1, NDEX

```

```

DUM1=AMU(LHAT,NP,J-1)

```

```

SUM1=SUM1 + DUM1

```

```

SUM2=SUM2 + DUM1*(-1.)**(NP +1)

```

```

IF(NP.EQ.NHAT +1) GOTO 20

```

```

SUM3=SUM3 + DUM1*2.*COMEGA*(NP-1)**2/((NP-1)**2 -NHAT**2)

```



```

1*(1. - (-1.)** (NP + NHAT - 1))
20 CONTINUE
  A150=BETA1*AK1/PSI(DUMMY)/EPSIZN(LHAT,MHAT,NHAT,ALENGTH,RLMDA)
  A151=BETAN*GAMMA*COMEGA*((-1.)**NHAT)*SUM2*FNORM(LHAT,MHAT,NHAT,
1RLMDA,ALENGTH)/EPSIZN(LHAT,MHAT,NHAT,ALENGTH,RLMDA)
  A152=(-1.)*AMACH*SUM3*FNORM(LHAT,MHAT,NHAT,RLMDA,ALENGTH)/EPSIZN(
1LHAT,MHAT,NHAT,ALENGTH,RLMDA)
  A153=BETAC*FNORM(LHAT,MHAT,NHAT,RLMDA,ALENGTH)*BESSEL(MHAT+1,LHAT)
1*SUM4/EPSIRZN(LHAT,MHAT,NHAT,ALENGTH,RLMDA)
  A155=(AK1/PSI(DUMMY) + GAMMA*COMEGA*FNORM(LHAT,MHAT,NHAT,RLMDA,
1ALENGTH)*SUM1)/EPSIZN(LHAT,MHAT,NHAT,ALENGTH,RLMDA)
  BETAIS(J)=(A150 - A151 - A152 - A153)/A155
  WRITE(6,100)J, BETAIS(J)
  AN = 1. / GAMMA - BETAIS(J) / AMACH
  WRITE(6,101) AN
  JS = J
  A150=BETAIS(J)-BETAIS(J-1)
  IF( ABS(REAL(A150)/REAL(BETAIS(J-1))) .LE.ERROR1 .AND. ABS(AIMAG(A15
10)/AIMAG(BETAIS(J-1))) .LE.ERROR2) GO TO 2
  RETURN
2 ISET = 1
  IF ( REAL(AN).GT.1.8.OR.AIMAG(AN).GT.1.0)CALL EXIT
  RETURN
100 FORMAT('0 BETA1(' ,12,' ) = ',2G21.14)
101 FORMAT('+' ,70X,' N = ',2G21.14,' |')
END
SUBROUTINE CALCA4( A4, A5 )
  COMPLEX BETA1, BETA2, BETAN, BETAC, BETA1, BETAW1, OMEGA, C, AK1,
1 AK2, PSI2
  COMPLEX A4, A5, PSI, DUMMY, G1, G2
  COMMON / BLKA / BETA1, BETA2, AMACH, GAMMA, OMEGA, ALENGTH, C, AK1
1, AK2, BETAN, RLMDA, BETA1, BETAC, BETAW1, LHAT, MHAT, NHAT,
1 PSI2,X1, X2
  A4 = AK1/EPSIZN(LHAT,MHAT,NHAT,ALENGTH,RLMDA)/PSI(DUMMY)
  A5=BETAC*(G1(X2,NHAT)-G1(X1,NHAT))/EPSIKAT(LHAT,MHAT,NHAT,ALENGTH,
1RLMDA)/PSI(DUMMY)
  RETURN
END
SUBROUTINE CALMU( JP )
  COMPLEX AMU,G1,G2,PSI,DUMMY,FNORM,A,DUM3,C12
  COMPLEX DUM1,DUM2,BETAIS,SUMS,S,COMEGA,SUM1,SUM2,SUM3,SUM4
  COMPLEX BETA1, BETA2, BETAN, BETAC, BETA1, BETAW1, OMEGA, C, AK1,
1AK2, PSI2

```

```

COMMON / BLKA / BETA1, BETA2, AMACH, GAMMA, OMEGA, ALENGTH, C, AK1
1, AK2, BETAN, RLMDA, BETA1, BETAC, BETAWI, LHAT, MHAT, NHAT,
1PS12,X1,X2/BLKB/AMU(10,30,29),BETAIS(30),A
COMMON C12(30,30),ISET,LDEX,NDEX,ERROR1,ERROR2
ISET = 0
DO 50 L = 1, LDEX
RLMDA1= BESPRIM(MHAT+1,L)
AC= BESSEL(MHAT+1,LHAT)/BESSEL(MHAT+1,L)
DO 50 NX = 1, NDEX
N=NX-1
IF(L.EQ.LHAT.AND.N.EQ.NHAT) GOTO 40
DUM1= CMPLX(0.,0.)
IF(L.EQ.LHAT) DUM1=(BETA1-BETAWI)*AK1/(EPSIZN(LHAT,MHAT,N,ALLENGTH,
1RLMDA1))
DUM1=A*(BETAC*(G1(X2,N)-G1(X1,N))/EPSIKAT(LHAT,MHAT,N,ALLENGTH,RLMD
1A1))*AC+DUM1)
DUM2=DUM1/((OMEGA**2-ETA(LHAT,MHAT,NX,ALLENGTH,RLMDA1))*PS1(DUMMY))
GOTO 50
40 DUM2=1.- A
50 AMU(L,NX,1)=DUM2/FNORM(LHAT,MHAT,NHAT,RLMDA,ALLENGTH)
NX = 1
COMEGA=CMPLX(-A*MAG(OMEGA),REAL(OMEGA))
DUM1=CMPLX(0.0,0.0)
DUM2=CMPLX(0.0,0.0)
N = NHAT
NX = NHAT + 1
DO 2 NY = 1, NDEX
NP=NY-1
IF(N.EQ.NP) 8,7
7 C12(NX,NY)=GAMMA/2./(N**2-NP**2)*(ALENGTH*COMEGA/3.1415926*((N+NP)
1*(SIN((N-NP)*3.1415926*X2/ALENGTH)-SIN((N-NP)*3.1415926*X1/ALENGTH
1)))+(N-NP)*(SIN((N+NP)*3.1415926*X2/ALENGTH)-SIN((N+NP)*3.1415926*X
11*ALENGTH))) -AMACH*NP*((NP+N)*(COS((NP-N)*3.1415926*X2/ALENGTH)-CO
1S((NP-N)*3.1415926*X1/ALENGTH)))+(NP-N)*(COS((NP+N)*3.1415926*X2/AL
1LENGTH)-COS((NP+N)*3.1415926*X1/ALENGTH)))
GO TO 2
8 IF(NP.EQ 0)9,10
9 C12(NX,NY)=(X2-X1)*COMEGA*GAMMA
GO TO 2
10 C12(NX,NY)=GAMMA*((SIN(2.*N*3.1415926*X2/ALENGTH)-SIN(2.*N*3.1415
1926*X1/ALENGTH))/4./N/3.1415926*ALENGTH+(X2-X1)/2.)*COMEGA-AMACH/2
1.*(SIN(N*3.1415926*X2/ALENGTH)**2-SIN(N*3.1415926*X1/ALENGTH)**2))
2 CONTINUE

```

```

CALL BETA1J( 2 )
IF(JP.EQ.1) RETURN
DO 1 NX = 1 , NDEX
N = NX - 1
DO 1 NY = 1 , NDEX
NP=NY-1
IF(N.EQ.NP) 3,4
4 C12(NX,NY)=GAMMA/2./(N**2-NP**2)*(ALENGTH*COMEGA/3.1415926*((N+NP)
1*(SIN((N-NP)*3.1415926*X2/ALENGTH)-SIN((N-NP)*3.1415926*X1/ALENGTH
1))+(N-NP)*(SIN((N+NP)*3.1415926*X2/ALENGTH)-SIN((N+NP)*3.1415926*X
11*ALENGTH)))-AMACH*NP*((NP+N)*(COS((NP-N)*3.1415926*X2/ALENGTH)-CO
1S((NP-N)*3.1415926*X1/ALENGTH))+(NP-N)*(COS((NP+N)*3.1415926*X2/AL
1ELENGTH)-COS((NP+N)*3.1415926*X1/ALENGTH)))
GO TO 1
3 IF(NP.EQ.0)5,6
5 C12(NX,NY)=(X2-X1)*COMEGA*GAMMA
GO TO 1
6 C12(NX,NY)=GAMMA*((SIN(2.*N*3.1415926*X2/ALENGTH)-SIN(2.*N*3.1415
1926*X1/ALENGTH))/4./N/3.1415926*ALENGTH+(X2-X1)/2.)*COMEGA-AMACH/2
1.*(SIN(N*3.1415926*X2/ALENGTH)**2-SIN(N*3.1415926*X1/ALENGTH)**2))
1 CONTINUE
DO 60 J=2,JP
DO 80 LS = 1 , LDEX
DO 80 NX = 1 , NDEX
NS=NX-1
RLMDA2=BESPRIM( MHAT + 1, LS)
DUM3 = BETAC*EPSIZN(LHAT,MHAT, NS ,ALENGTH,RLMDA)*BESSEL(MHAT+1,
1LHAT)/EPSIKAT(LS,MHAT,NS,ALENGTH,RLMDA2)/BESSEL(MHAT+1,LS)
DUM1 = CMPLX( 0.0, 0.0 )
SUMS=CMPLX(0.,0.)
IF( LS .EQ. LHAT .AND. NS .EQ. MHAT ) 15, 16
15 AMU(LHAT, NX,J) = CMPLX( 0.0 , 0.0 )
GO TO 80
16 SUM1=SUM2=SUM3=SUM4=CMPLX(0.0,0.0)
DO 90 LP = 1 , LDEX
RLMDA3=BESSEL(MHAT +1,LP)
RLMDA4=BESSEL(MHAT +1,LHAT)
DO 90 NY = 1 , NDEX
SUM4=SUM4 + AMU(LP,NY,J-1)*C12(NX,NY)
90 CONTINUE
SUM4=SUM4*DUM3*RLMDA3/RLMDA4
DO 21 NP = 1 , NDEX
DUM1=AMU(LS,NP,J-1)

```

```

SUM1=SUM1 +DUM1
SUM2=SUM2 + DUM1*(-1.)**(NP +1)
IF(NP.EQ.NX) GOTO 21
SUM3=SUM3 + DUM1*2.*COMEGA*(NP-1)**2 *(1.-(-1.)**(NP+NX))/(
1(NP-1)**2 -NS**2 )
21 CONTINUE
SUM1=BETAIS(J)*GAMMA*COMEGA*SUM1
SUM2=BETAN*GAMMA*COMEGA*(-1.)**NS*SUM2
SUM3=SUM3 + AMACH*(3.1415926*NS)**2./2./ALENGTH*AMU(LS,NX,J-1)
SUM3=(-1.)*AMACH*SUM3
DUM1=CMPLX(0.0,0.0)
IF(LS.EQ.LHAT) DUM1=(BETAIS(J) - BETAW1)*AK1
DUM1=DUM1 +DUM3*(G1(X2,NS) -G1(X1,NS))
DUM1=DUM1/PSI(DUMMY)/FNORM(LHAT,MHAT,NHAT,RLMDA,ALENGTH)
AMU(LS,NX,J)=(DUM1 +SUM1 +SUM2 +SUM3 + SUM4)/(OMEGA**2 - ETA(LHAT
1,MHAT,NX,ALENGTH,BESPRIM(MHAT+1,LS)))/EPSIZN(LHAT,MHAT,NS,ALENGTH,
2RLMDA)
80 CONTINUE
CALL BETA1J( J + 1 )
IF ( ISET .NE. 0 ) GO TO 17
60 CONTINUE
17 CONTINUE
JP = J
RETURN
END
FUNCTION EPSIKAT(L,M,N,ALENGTH,RLMDA)
DUM1 = ALENGTH
IF( N .NE. 0) DUM1 = DUM1/2.
IF( M .EQ. 0) GOTO 1
EPSIKAT = (0.5-M *M / (2.*RLMDA*RLMDA))*DUM1
RETURN
1 EPSIKAT = DUM1/2.
RETURN
ENTRY EPSIZN
IF( N .EQ. 0 ) GO TO 2
EPSIKAT= ALENGTH / 2.
RETURN
2 EPSIKAT= ALENGTH
RETURN
ENTRY ETA
EPSIKAT = (N-1)*(N-1) * 3.1415926 *3.1415926 / (ALENGTH * ALENGTH)
1+RLMDA * RLMDA
RETURN

```

```

END
FUNCTION EPSIRZN(L,M,N,ALENGTH,RLMDA)
COMPLEX FNORM,DUM2
DUM1 = 1.
IF(M.EQ.0) DUM1 = .5
DUM2=FNORM(L,M,N,RLMDA,ALENGTH)**2
EPSIRZN=DUM1 *REAL(DUM2)/3.1415926
RETURN
END
COMPLEX FUNCTION FNORM(L,M,N,RLMDA,ALENGTH)
DUM1 = 3.1415926
IF( M .EQ. 0 ) DUM1 = 6.2831852
DUM1=DUM1*EPSIKAT(L,M,N,ALENGTH,RLMDA)*BESSEL(M+1,L)**2
FNORM=CMPLX(DUM1,0.0)
FNORM= CSQRT(FNORM)
RETURN
END
COMPLEX FUNCTION G1 (X,N)
COMPLEX BETA1, BETA2, BETAN, BETAC, BETA1, BETAW1, OMEGA, C, AK1,
1 AK2, PSI2
COMPLEX DUM1, GDUM, BETA
COMMON / BLKA / BETA1, BETA2, AMACH, GAMMA, OMEGA, ALENGTH, C, AK1
1, AK2, BETAN, RLMDA, BETA1, BETAC, BETAW1, LHAT, MHAT, NHAT,
1 PSI2,X1, X2
GDUM(A,DUM1,BETA,OMEGA,AMACH,X) = (OMEGA+AMACH*BETA)/(A**2-BETA**2
1 )*(CEXP(DUM1*X)*(DUM1 *COS(A*X)+A*SIN(A*X))-DUM1)
IF( X .EQ. 0.0 ) GO TO 1
A = N*3.1415926/ALENGTH
BETA = BETA1
DUM1 = CMPLX(-AIMAG(BETA1),REAL(BETA1))
G1 = GDUM(A,DUM1,BETA,OMEGA,AMACH,X)
IF( N .EQ. 0 .AND. CABS( BETA2) .LE. 1.E-10 ) GO TO 2
BETA = BETA2
DUM1 = CMPLX(-AIMAG(BETA2),REAL(BETA2))
G1 = GAMMA * (G1 + C * GDUM(A,DUM1,BETA,OMEGA,AMACH,X))
G1 = CMPLX( -AIMAG(G1),REAL(G1))
RETURN
1 G1 = CMPLX(0.0,0.0)
RETURN
2 BETA = C * OMEGA * X
G1 = GAMMA * ( G1 + BETA )
G1 = CMPLX( -AIMAG(G1), REAL(G1))
RETURN

```

```

END
COMPLEX FUNCTION G2(N)
COMPLEX BETA1, BETA2, BETAN, BETAC, BETA1, BETAW1, OMEGA, C, AK1,
1 AK2, PS12
COMPLEX DUM1, BETA, GBUM, DUM
COMMON / BLKA / BETA1, BETA2, AMACH, GAMMA, OMEGA, ALENGTH, C, AK1
1, AK2, BETAN, RLMDA, BETA1, BETAC, BETAW1, LHAT, MHAT, NHAT,
1 PS12, X1, X2
GBUM(BETA, DUM1, N, AMACH, OMEGA, ALENGTH) = -(AMACH*BETA*BETA+2.*OMEGA
1 *BETA)/((N * 3.1415926 / ALENGTH)**2 - BETA**2) * (CEXP(DUM1*
1 ALENGTH) * DUM1 * (-1.)**(N+2) - DUM1)
DUM(DUM1, ALENGTH, NHAT) = CEXP(DUM1*ALENGTH)*(-1.)**(NHAT+2)-1.
BETA = BETA1
DUM1 = CMPLX(-AIMAG(BETA1), REAL(BETA1))
G2 = GBUM(BETA, DUM1, N, AMACH, OMEGA, ALENGTH)
IF( N .EQ. 0 .AND. CABS( BETA2) .LE. 1.E-10 ) RETURN
BETA = BETA2
DUM1 = CMPLX(-AIMAG(BETA2), REAL(BETA2))
G2 = G2 + C * GBUM(BETA, DUM1, N, AMACH, OMEGA, ALENGTH)
RETURN
ENTRY PSI
DUM1 = CMPLX(-AIMAG(BETA1), REAL(BETA1))
G2 = DUM1*DUM(DUM1, ALENGTH, NHAT)/(NHAT**2*3.1415926**2/ALENGTH**2
1 -BETA1**2)
IF( NHAT .EQ. 0 .AND. CABS( BETA2) .LE. 1.E-10 ) GO TO 3
DUM1 = CMPLX(-AIMAG(BETA2), REAL(BETA2))
G2 = ( G2 + C*DUM1*DUM(DUM1, ALENGTH, NHAT)/(NHAT**2*3.1415926**2/
1 ALENGTH**2-BETA2**2))/EPSIZN(LHAT, MHAT, NHAT, ALENGTH, RLMDA)
RETURN
3 G2 = ( G2 + C * ALENGTH ) / EPSIZN(LHAT, MHAT, NHAT, ALENGTH, RLMDA)
RETURN
END

```

THE FOLLOWING IS AN EXAMPLE OF THE PUNCHED CARD INPUT.

REFERENCE	0.90	0.00	2.70	0.33	1.20	0.9166	0.00
5.0	0.0	0.0	0.90	0.01	0.01	1 1 0 3 30NO	
0.0500000	0.0000000	0.9000000	0.0000000				

THIS IS ENGINE NUMBER REFERENCE
 THE COEFFICIENT MATRIX IS 3 X 30
 THE MACH NUMBER IS .330000000000000
 THE RATIO OF SPECIFIC HEATS IS 1.20000000000000
 THE FREQUENCY IS 1.6570654020000 0.
 THE LENGTH OF THE COMBUSTOR IS 2.70000000000000
 THE PRIMARY MODE ASSUMED IS LHAT = 1 MHAT = 1 NHAT = 0
 THE LINER BEGINS AT 0.0000 AND ENDS AT .9000
 W/WO = .900000000000000 0.
 A = 1.000000000000000 0.
 BETAN = 2.747800000000000E-02 0.
 G = .916600000000000 0.
 BETAC = .166666666666667 0.
 K = 5.000000000000000 0.
 BETAWI = .28047988577675 .23813090794998
 N = -1.66057144750020E-02 -.72160881196963 I
 BETAWID = .28047988577675 .23813090794997
 N = -1.66057144750020E-02 -.72160881196961 I
 BETA1(1) = -3.62072818079238E-02 .16649307640463
 N = .94305236911492 -.50452447395341 I
 BETA1(2) = 7.57432135587427E-03 .29698397044242
 N = .81038084437614 -.89995142558308 I
 BETA1(3) = 3.47010788505651E-02 .28016921968467
 N = .72817854893768 -.84899763540808 I
 BETA1(4) = 3.02237853398196E-02 .27965997230247
 N = .74174610503085 -.84745446152262 I
 BETA1(5) = 3.20665167674021E-02 .28192424117869
 N = .73616207040181 -.85431588235965 I
 BETA1(6) = 3.27799204196444E-02 .28157699072313
 N = .73400024115259 -.85326360825190 I
 BETA1(7) = 3.29116946035384E-02 .28169303136132
 N = .73360092544382 -.85361524654944 I